ARL-STRUC-R-434

AR-005-548

DEPARTMENT OF DEFENCE

DEFENCE SCIENCE AND TECHNOLOGY ORGANISATION

AERONAUTICAL RESEARCH LABORATORY

MELBOURNE, VICTORIA

Aircraft Structures Report 434

STRESSES AND STRAINS IN A COLD-WORKED ANNULUS

by

G.S. Jost

Approved for Public Release

SEPTEMBER 1988

AR-005-548

DEPARTMENT OF DEFENCE
DEFENCE SCIENCE AND TECHNOLOGY ORGANISATION
AERONAUTICAL RESEARCH LABORATORY

Aircraft Structures Report 434

STRESSES AND STRAINS IN A COLD-WORKED ANNULUS

by

G.S. Jost

SUMMARY

Analytically-derived plane strain stresses and strains in an annulus pressurised sufficiently to cause plastic flow are given. Unloading giving rise to reyielding around the bore is then examined, along with the effect of reaming. Cold-working is then included in the analysis in terms of interference between mandrel and hole. Finally, comparisons of stress and strain predictions are made with those from a finite element analysis.

POSTAL ADDRESS: Director, Aeronautical Research Laboratory,
P.O. Box 4331, Melbourne, Victoria, 3001, Australia

NOMENCLATURE

a	hole radius
b	outer radius of annulus
c	elasto-plastic radius resulting from cold-expansion
e	base of natural logarithms
E	Young's modulus of annulus material
E_m	Young's modulus of mandrel material
g	ratio E/E_m
I	radial interference
p	pressure
r	radius
u	displacement
α	$2 \ln (c/a) + 1 - (c/b)^2$
γ	Lame constant (equation 4)
δ	change (applied to radius)
ϵ	strain
λ	dimensionless interference, I/a
ν	Poisson's ratio
ρ	reyield radius
σ	stress

Subscripts

a	at bore
c	at elasto-plastic radius
m	mandrel
o	yield
r	radial
z	axial
θ	circumferential

Superscript

$'$	radius after reaming

1. INTRODUCTION

The fatigue process in aircraft structures is very often associated with the presence of stress concentrations of one kind or another, and fastener holes represent by far the most numerous such feature in any mainly metallic structure. For some time now substantial attention has been given to methods for improving the fatigue behaviour of structures containing holes, one of the most successful of these methods being the cold-expansion process[1]. In common with other mechanical means, hole cold-expansion achieves its quite dramatic effect (life improvement factors typically of the order of two to five)[2] by modifying the local stress field[3] to become benign so far as the fatigue process is concerned.

In the cold-expansion process the hole is expanded by the passage of an oversize or interference-fit tapered mandrel through the hole, a sleeve or protective bush being used to prevent the possibility of scoring or galling. As the mandrel enters the hole, the surrounding material is first expanded (typically of the order of 3 to 5% of diameter) causing local yield to occur. As the mandrel leaves the hole the surrounding elastically deformed material forces a reduction in hole diameter from the fully expanded size, and this reduction can be such as to cause plastic flow in the reverse or negative sense. Of course the extent (i.e. radius) of this reyielded zone is substantially less than that generated by the mandrel in enlarging the hole. The final stage in cold-working is usually the reaming of the hole to provide a precise diameter to receive a transition- or interference-fit fastener. It can be seen that the process results in a region of material surrounding the hole which is compressively stressed, and this is highly beneficial in delaying the onset of fatigue crack initiation and in reducing the rate of propagation of developing fatigue cracks. It is not until the growing crack tip reaches that region corresponding to a tensile circumferential stress field that the beneficial effect of the cold-working process is lost - this occurs typically at about 2 to 3 hole radii - and by that time the sought substantial increase in total fatigue life has already been achieved.

The analysis of this report relates to an axisymmetric thick-walled annulus under conditions of plane strain, pressurised and depressurised to simulate the cold-expansion process. The elasto-plastic pressurised cylinder has been much studied in the past [4-10] and this report makes no further contribution to this field per se. It does, however, focus the application of this work on pressurised cylinders to hole cold-expansion in annuli. Use is made of Hencky deformation theory, incompressible plastic flow and the von Mises yield criterion, all of which have previously been

applied to the elasto-plastic cylinder problem[11]. A recent paper on cold-expansion[12] also used these same assumptions. To the author's knowledge, however, no single source provides formulations of all of the quantities of interest relating to cold-expansion: it is for this reason that the present report has been prepared.

For the sake of convenience and completeness here, the derivations of all stresses, strains, elasto-plastic radii, etc are given for each of the three main cold-expansion stages as follows:

(a) mandrel fully in - hole fully expanded, plastic flow around hole
(b) mandrel removed - effect of elastic recovery, reyielding at hole
(c) effect of reaming - modification to stress and strain fields

Then, because cold-expansion is specified in terms of interference between mandrel and hole, rather than applied pressure, the relations between these for the various conditions are derived to permit recasting of the stress and strain equations in terms of interference.

Finally, a comparison is made between stress and strain predictions from the present report with those from a plane strain finite element study using incremental plasticity theory. The two sets of predictions show good agreement for the quantities of interest.

2. GENERAL RELATIONSHIPS

In the axisymmetric problem to be discussed, the radial, circumferential and axial directions are also the principal directions. All formulations are given in terms of these principal directions.

2.1 Elastic Region

For plane strain conditions ($\epsilon_z = 0$) the following general relationships hold[5]:

$$\epsilon_r = [\sigma_r - \nu\,(\sigma_\theta + \sigma_z)]/E = \frac{du_r}{dr}$$

$$\epsilon_\theta = [\sigma_\theta - \nu\,(\sigma_z + \sigma_r)]/E = \frac{u_r}{r} \qquad (1)$$

$$\epsilon_z = [\sigma_z - \nu\,(\sigma_r + \sigma_\theta)]/E = 0$$

From the last of these

$$\sigma_z = \nu(\sigma_r + \sigma_\theta) \tag{2}$$

Rearranging (1) to obtain stresses in terms of strains gives

$$\begin{aligned} \sigma_r &= \gamma \left[\epsilon_r + \frac{\nu}{1-\nu}\,\epsilon_\theta\right] \\ \sigma_\theta &= \gamma \left[\epsilon_\theta + \frac{\nu}{1-\nu}\,\epsilon_r\right] \\ \sigma_z &= \gamma \left[\epsilon_r + \epsilon_\theta\right] \end{aligned} \tag{3}$$

where γ is given by

$$\gamma = E\,\frac{1-\nu}{(1+\nu)(1-2\nu)} \tag{4}$$

2.2 Plastic Region

A substantial and extending literature exists on the intricacies of how to best represent plastic flow. All theories, of necessity, include approximations which better or worse suit a given application. In this report, for the sake of achievability in conjunction with practical usefulness, deformation plasticity theory is used. The following assumptions are made:

(a) Incompressibility - plastic flow occurs with no change in volume. This corresponds to Poisson's ratio becoming equal to one half.

(b) Plane strain - as before, $\epsilon_z = 0$, and from the Hencky equations[6] it follows that

$$\sigma_z = \tfrac{1}{2}\,(\sigma_r + \sigma_\theta) \tag{5}$$

and

$$\epsilon_r + \epsilon_\theta = 0 \tag{6}$$

These results also follow directly from (1) and (2) with $\nu = \frac{1}{2}$.

(c) Yield criterion - in terms of principal stresses, the von Mises criterion is given by

$$(\sigma_r - \sigma_\theta)^2 + (\sigma_\theta - \sigma_z)^2 + (\sigma_z - \sigma_r)^2 = 2\sigma_o^2$$

Substituting for σ_z from (5) gives

$$\sigma_r - \sigma_\theta = \pm \frac{2}{\sqrt{3}} \sigma_o \qquad (7)$$

(d) An elastic/perfectly-plastic stress-strain relationship is assumed in both positive and negative senses. Work hardening does not occur and the Bauschinger effect is not accounted for.

Because of these simplifications, incompatibilities do occur - in particular, because of the need for step changes in the values of ν across elasto-plastic boundaries. For practical purposes, however, these inconsistencies are usually either small in magnitude or affect quantities of secondary interest only.

3. STRESSES

In this section the principal stress distributions are given for the annulus first under internal pressure loading and then following removal of the pressure.

3.1 Loaded Annulus

The application of pressure to the bore of the annulus gives rise to three possible outcomes of interest:

(a) elastic expansion throughout
(b) expansion such that the material at the bore is about to yield - incipient yielding
(c) expansion such that a plastic zone extends from the bore to an elasto-plastic boundary, the surrounding material remaining elastic.

Each of these is now examined in turn.

3.1.1 Elastic Conditions Throughout

The equilibrium equation for an annulus under axisymmetric loading is given by[5]

$$\frac{d\sigma_r}{dr} + \frac{\sigma_r - \sigma_\theta}{r} = 0 \tag{8}$$

the solution of which is[5], for internal pressure loading p,

$$\sigma_r = - p \frac{(\frac{a^2}{r}) - (\frac{a^2}{b})}{1 - (\frac{a^2}{b})}$$

$$\sigma_\theta = p \frac{(\frac{a^2}{r}) + (\frac{a^2}{b})}{1 - (\frac{a^2}{b})} \tag{9}$$

and from (2),

$$\sigma_z = 2 \nu p \frac{(\frac{a^2}{b})}{1 - (\frac{a^2}{b})}$$

By way of example, these stress distributions for the case of $b/a = 5$ and $\nu = 1/3$ are shown in Fig. 2. Note that σ_z is constant across the section.

3.1.2 Incipient Plastic Flow

Increase in pressure in the bore eventually leads to the onset of plastic flow there. Substitution of (9) into (7) provides the pressure at which plastic deformation begins:

$$p_a = \sigma_o \frac{1 - (a/b)^2}{\sqrt{[3 + (1-2\nu)^2 (a/b)^4]}}$$

where the subscript denotes incipient plastic flow at $r = a$.

For practical values of a/b in the cold-expansion situation (no larger than one-half), the second term in the denominator above is quite negligible, so that, for practical purposes

$$p_a = \frac{\sigma_o}{\sqrt{3}} [1 - (\frac{a}{b})^2] = -\sigma_r \tag{10}$$

3.1.3 Stresses in Plastic Region

Further increase in pressure gives rise to an enlarging region of plastic flow around the hole, surrounded by a restraining elastic region beyond. The elastic region provides a constraint on the extent of plastic flow which is crucial to the effectiveness of the cold-expansion process in increasing fatigue life.

In the plastic region, as already noted at (7), the yield criterion becomes

$$\sigma_\theta - \sigma_r = \frac{2}{\sqrt{3}}\,\sigma_o \tag{11}$$

Substitution of (11) into the equilibrium equation (8), integrating, and noting that at $r = c$ the radial stress there is given by (10) with radius a replaced by c, leads to

$$\sigma_r = \frac{\sigma_o}{\sqrt{3}}\left[2 \ln \frac{r}{c} - 1 + \left(\frac{c^2}{b}\right)\right]$$

From (11)

$$\sigma_\theta = \frac{\sigma_o}{\sqrt{3}}\left[2 \ln \frac{r}{c} + 1 + \left(\frac{c^2}{b}\right)\right] \tag{12}$$

and from (5)

$$\sigma_z = \frac{\sigma_o}{\sqrt{3}}\left[2 \ln \frac{r}{c} + \left(\frac{c^2}{b}\right)\right]$$

Equations (12) give the stress distributions in the plastic region ($a \leq r \leq c$) of a pressurised annulus surrounded by an elastic region between radii c and b.

The pressure (applied at $r = a$) to cause yielding to radius c is found from the first of (12) as

$$p_c = (-\sigma_r)_c = \frac{\sigma_o}{\sqrt{3}}\left[2 \ln \left(\frac{c}{a}\right) + 1 - \left(\frac{c^2}{b}\right)\right] \tag{13}$$

$$= \frac{\sigma_o}{\sqrt{3}}\,\alpha$$

where

$$\alpha = 2 \ln \frac{c}{a} + 1 - \left(\frac{c^2}{b}\right) \tag{14}$$

3.1.4 Stresses in Elastic Region

The stresses in the elastic region are found from (9) by substituting for p the expression (10) and by changing all a to c. Thus

$$\sigma_r = \frac{\sigma_o}{\sqrt{3}} \left[-\left(\frac{c^2}{r}\right) + \left(\frac{c^2}{b}\right)\right]$$

$$\sigma_\theta = \frac{\sigma_o}{\sqrt{3}} \left[\left(\frac{c^2}{r}\right) + \left(\frac{c^2}{b}\right)\right] \qquad (15)$$

$$\sigma_z = \frac{2\nu\sigma_o}{\sqrt{3}} \left(\frac{c^2}{b}\right)$$

Equations (15) give the stress distributions in the elastic region ($c \leq r \leq b$) of a pressurised annulus in which the region $a \leq r \leq c$ has undergone plastic flow. Note that, as before, σ_z is constant in this region, and for b large, $\sigma_z \to 0$.

The elasto-plastic stress distributions across the section for the same case as before, and with $b/c = 2$, are shown in Fig. 3. This shows the discontinuity in σ_z at $r = c$ caused by the step-change in ν at the elasto-plastic boundary - it decreases with increasing b and disappears when b becomes infinite. More sophisticated[7] and more complicated analyses introduce second-order terms to eliminate this. In the context of this report, third-direction parameters are given for completeness only.

3.2 Unloaded Annulus

Upon removal of the pressure in the bore, recovery of the material takes place under the action of the outer elastically stressed material. The elastic recovery is quantified by the superposition of the elastic equations (9) with an appropriate sign change. The extent of the unloading is governed by the requirement that the residual radial stress at the bore of the hole must be zero. In general, this gives rise to another (reyielded) plastic zone in the neighbourhood of the bore, of much smaller radius than that occurring under load. Alternatively, since the pressure applied to the hole in Section 3.1 is given by (13), this is precisely the value required to be substituted for p in (9) to establish the residual stress fields by subtraction of (9) from (12) and (15).

Three outcomes are possible:

(a) elastic unloading across the full width of the annulus.

(b) as above, but with incipient reyielding at the bore.

(c) as above, but with a finite reyielded region surrounding the bore.

It is assumed in the following that loading of the annulus has given rise to a fully elasto-plastic situation as detailed in Sections 3.1.3 and 3.1.4 (Fig. 3). For the elastic and incipient plastic loaded situations of Sections 3.1.1 and 3.1.2 only elastic unloading is possible, leaving no residual stresses.

3.2.1 Elastic Recovery - No Reyielding

When the recovery from the loaded configuration is wholly elastic, no further plastic flow is induced at the bore. In this case the residual stresses are found as outlined above.

For the zone $a \leq r \leq c$

$$\sigma_r = \frac{\sigma_o}{\sqrt{3}} \left\{ \left[2 \ln \frac{r}{c} - 1 + \left(\frac{c^2}{b}\right) \right] + \alpha \frac{\left(\frac{a^2}{r}\right) - \left(\frac{a^2}{b}\right)}{1 - \left(\frac{a^2}{b}\right)} \right\}$$

$$\sigma_\theta = \frac{\sigma_o}{\sqrt{3}} \left\{ \left[2 \ln \frac{r}{c} + 1 + \left(\frac{c^2}{b}\right) \right] - \alpha \frac{\left(\frac{a^2}{r}\right) + \left(\frac{a^2}{b}\right)}{1 - \left(\frac{a^2}{b}\right)} \right\} \qquad (16)$$

$$\sigma_z = \frac{\sigma_o}{\sqrt{3}} \left\{ \left[2 \ln \frac{r}{c} + \left(\frac{c^2}{b}\right) \right] - 2\nu\, \alpha \frac{\left(\frac{a}{b}\right)^2}{1 - \left(\frac{a^2}{b}\right)} \right\}$$

For the zone $c \leq r \leq b$

$$\sigma_r = \frac{\sigma_o}{\sqrt{3}} \left\{ \left[-\left(\frac{c^2}{r}\right) + \left(\frac{c^2}{b}\right) \right] + \alpha \frac{\left(\frac{a^2}{r}\right) - \left(\frac{a^2}{b}\right)}{1 - \left(\frac{a^2}{b}\right)} \right\}$$

$$\sigma_\theta = \frac{\sigma_o}{\sqrt{3}} \left\{ \left[\left(\frac{c^2}{r}\right) + \left(\frac{c^2}{b}\right) \right] - \alpha \frac{\left(\frac{a^2}{r}\right) + \left(\frac{a^2}{b}\right)}{1 - \left(\frac{a^2}{b}\right)} \right\} \qquad (17)$$

$$\sigma_z = \frac{2\nu\sigma_o}{\sqrt{3}} \left\{ \left(\frac{c^2}{b}\right) - \alpha \frac{\left(\frac{a^2}{b}\right)}{1 - \left(\frac{a^2}{b}\right)} \right\}$$

where, as noted at (14),

$$\alpha = 2 \ln \frac{c}{a} + 1 - \left(\frac{c^2}{b}\right)$$

Equations (16) and (17) give the residual stresses in an annulus in which loading has caused yield to radius c.

3.2.2 Elastic Recovery - Incipient Reyield at Bore

In this case, since $\sigma_r = 0$ at the bore, the yield criterion (7) becomes

$$\sigma_\theta = -\frac{2}{\sqrt{3}} \sigma_o \tag{18}$$

Substituting for σ_θ from (18) in the second of (16), and putting r = a there gives

$$-\frac{2}{\sqrt{3}} \sigma_o = \frac{\sigma_o}{\sqrt{3}} \left\{ \left[2 \ln \frac{a}{c} + 1 + \left(\frac{c^2}{b}\right) \right] - \alpha \frac{1 + \left(\frac{a^2}{b}\right)}{1 - \left(\frac{a^2}{b}\right)} \right]\right\}$$

from which

$$2 \ln \frac{c}{a} + 1 - \left(\frac{c^2}{b}\right) = 2 \left[1 - \left(\frac{a^2}{b}\right)\right] \tag{19}$$

Equation (19) specifies the condition under which reyield will initiate at the bore on unloading in terms of the elasto-plastic radius c.

Rearranging (19) as

$$\left(\frac{b^2}{a}\right) = \frac{\left(\frac{c^2}{a}\right) - 2}{2 \ln \frac{c}{a} - 1} \tag{20}$$

and solving for b/a provides the locus of incipient reyielding shown in Fig. 4. For b/a less than 2.22 reyielding can never occur, and reyielding will never occur when c/a is less than 1.65. The first condition is a geometric requirement, the

second a loading requirement: there has to be sufficient surrounding material available to impose the necessary recovery on unloading, and the extent of the load-induced plastic zone has to be such that reyield can occur on unloading. For b/a greater than 22.2, reyielding always occurs from a fully plastic expansion, i.e. from the condition c/a = b/a.

3.2.3 Unloading giving rise to Reyielded Zone

In this case unloading gives rise to a reyielded zone around the bore of radius ρ, as indicated diagramatically in Fig. 1(b).

For the zone $a \leq r \leq \rho$

Stresses in the reyielded region are readily found. Substitution of (11) into the equilibrium equation (8), integrating, and noting that $\sigma_r = 0$ at $r = a$ provides the following

$$\sigma_r = -\frac{2\sigma_o}{\sqrt{3}} \ln \frac{r}{a}$$

$$\sigma_\theta = -\frac{2\sigma_o}{\sqrt{3}} \left[1 + \ln \frac{r}{a}\right] \qquad (21)$$

$$\sigma_z = -\frac{\sigma_o}{\sqrt{3}} \left[1 + 2 \ln \frac{r}{a}\right]$$

For the zone $\rho \leq r \leq c$

Stresses in this region may be written down directly from (16) after first making the substitution (19) for α and then replacing a by ρ:

$$\sigma_r = \frac{\sigma_o}{\sqrt{3}} \left\{\left[2 \ln \frac{r}{c} - 1 + \left(\frac{c^2}{b}\right)\right] + 2 \left[\left(\frac{\rho^2}{r}\right) - \left(\frac{\rho^2}{b}\right)\right]\right\}$$

$$\sigma_\theta = \frac{\sigma_o}{\sqrt{3}} \left\{\left[2 \ln \frac{r}{c} + 1 + \left(\frac{c^2}{b}\right)\right] - 2 \left[\left(\frac{\rho^2}{r}\right) + \left(\frac{\rho^2}{b}\right)\right]\right\} \qquad (22)$$

$$\sigma_z = \frac{\sigma_o}{\sqrt{3}} \left\{\left[2 \ln \frac{r}{c} + \left(\frac{c^2}{b}\right)\right] - 2\nu \left(\frac{\rho^2}{b}\right)\right\}$$

In this region σ_r reaches a minimum when $r/\rho = \sqrt{2}$, at which point $\sigma_r = \sigma_\theta$. This is also the region in which σ_θ changes sign: that occurs when r satisfies

$$\ln \frac{ar}{\rho^2} = \left(\frac{\rho}{r}\right)^2 \tag{23}$$

For the zone $c \leq r \leq b$

Stresses in this region may also be written down directly. From (17), after substituting (19) for α and replacing a by ρ:

$$\sigma_r = \frac{\sigma_o}{\sqrt{3}} \left\{\left[-\left(\frac{c}{r}\right)^2 + \left(\frac{c}{b}\right)^2\right] + 2\left[\left(\frac{\rho}{r}\right)^2 - \left(\frac{\rho}{b}\right)^2\right]\right\}$$

$$\sigma_\theta = \frac{\sigma_o}{\sqrt{3}} \left\{\left[\left(\frac{c}{r}\right)^2 + \left(\frac{c}{b}\right)^2\right] - 2\left[\left(\frac{\rho}{r}\right)^2 + \left(\frac{\rho}{b}\right)^2\right]\right\} \tag{24}$$

$$\sigma_z = \frac{\sigma_o}{\sqrt{3}} 2\nu \left[\left(\frac{c}{b}\right)^2 - 2\left(\frac{\rho}{b}\right)^2\right]$$

Equations (21) to (24) contain the unknown reyield radius ρ. Radius ρ is not independent, but depends upon the extent of prior yielding, c, and the geometry of the annulus. Its magnitude is, however, readily found.

3.2.4 Relationship between Yield Radii c and ρ

The results of the previous Section provide a ready means of establishing the relationship between c and ρ. By equating like stresses (σ_r or σ_θ) from (21) and (22) at $r = \rho$ there results

$$2 \ln \frac{ac}{\rho^2} + 1 - \left(\frac{c}{b}\right)^2 = 2\left[1-\left(\frac{\rho}{b}\right)^2\right] \tag{25}$$

This the reyield equivalent of the incipient reyield case of Section 3.2.2 and reduces to (19) when $\rho = a$. Equation (25) provides the sought relationship between ρ and c. As before, (25) may be rearranged as

$$\left(\frac{b}{\rho}\right)^2 = \frac{\left(\frac{c}{\rho}\right)^2 - 2}{2 \ln \frac{a}{\rho}\frac{c}{\rho} - 1} \tag{26}$$

The plot of (26) is shown in Fig. 5, which is an extension of Fig. 4 for the incipient reyield case. The reyield regime now has the additional information shown in terms of loci of the parameters ρ/a and c/ρ. It is seen that, for a given geometry b/a, as the yield radius c (or c/a) increases - corresponding to increasing load at the bore in the first place - the generated reyield radius ρ (or ρ/a) also increases, as expected. Also, increasing c/a gives rise to increasing c/ρ, the ratio of the reyield radii.

For b large, from (26)

$$\rho = \sqrt{(ac)}/e^{\frac{1}{4}}$$

For the loaded example considered earlier and shown in Fig. 3, the unloaded equivalent may now be evaluated. By solving (26) for $b/a = 5$ and $c/a = 2.5$ (or by scaling from Fig. 5) the corresponding $\rho/a = 1.19$, giving $c/\rho = 2.10$. Equations (21) to (24) may now be evaluated, the plots being shown in Fig. 6. Once again the inconsistencies in z-direction stresses across the elasto-plastic boundaries are apparent. Notice, however, the significant extent of the circumferential stress field below zero (from (26) this extends to $r/a = 2.01$) and the size of the reyielded region ($\rho/a = 1.19$) : both aspects play a major part in delaying and then slowing fatigue crack growth from the hole.

3.3 Effect of Reaming

For engineering reasons it is common to ream holes after cold-expansion: the final radius of the hole thereby becomes slightly larger than that immediately after cold-working. The effect of this on the stress fields may be considered as follows: the reaming process clearly exerts no influence on the loaded situation - all loaded stresses remain as before. But consider now that the bore of the loaded annulus is enlarged so that on unloading, recovery occurs on the basis of this larger radius: this is exactly the situation existing after reaming. The effect is found simply by substituting a' ($= a + \delta a$) for a in the unloading components of the equations*.

---

* Care is required in tracking radii here. In evaluating effects, the reamed radius should be compared with the post-cold-expanded, pre-reamed value (see Section 5). The effect of reaming must be calculated on this small difference in radii, not on the larger difference between final ream radius and initial, unloaded radius.

As anticipated, reaming marginally relaxes the desirable effects of the residual stress distributions effected by cold-working.

3.3.1 Reaming where no Reyield has occurred

This case is that of all-elastic unloading. From Section 3.2.1 the required solutions are found by replacing radius a in (16) and (17) with a' in the elastic unloading components, i.e. those with the α multiplier.

For the zone $a' \leq r \leq c$

$$\sigma'_r = \frac{\sigma_o}{\sqrt{3}} \left\{ \left[2 \ln \frac{r}{c} - 1 + \left(\frac{c^2}{b}\right) \right] + \alpha' \frac{\left(\frac{a'}{r}\right)^2 - \left(\frac{a'}{b}\right)^2}{1 - \left(\frac{a'}{b}\right)^2} \right\}$$

$$\sigma'_\theta = \frac{\sigma_o}{\sqrt{3}} \left\{ \left[2 \ln \frac{r}{c} + 1 + \left(\frac{c^2}{b}\right) \right] - \alpha' \frac{\left(\frac{a'}{r}\right)^2 + \left(\frac{a'}{b}\right)^2}{1 - \left(\frac{a'}{b}\right)^2} \right\} \qquad (27)$$

$$\sigma'_z = \frac{\sigma_o}{\sqrt{3}} \left\{ \left[2 \ln \frac{r}{c} + \left(\frac{c^2}{b}\right) \right] - 2\nu\alpha' \frac{\left(\frac{a'}{b}\right)^2}{1 - \left(\frac{a'}{b}\right)^2} \right\}$$

For the zone $c \leq r \leq b$

$$\sigma'_r = \frac{\sigma_o}{\sqrt{3}} \left\{ \left[-\left(\frac{c^2}{r}\right) + \left(\frac{c^2}{b}\right) \right] + \alpha' \frac{\left(\frac{a'}{r}\right)^2 - \left(\frac{a'}{b}\right)^2}{1 - \left(\frac{a'}{b}\right)^2} \right\}$$

$$\sigma'_\theta = \frac{\sigma_o}{\sqrt{3}} \left\{ \left[\left(\frac{c^2}{r}\right) + \left(\frac{c^2}{b}\right) \right] - \alpha' \frac{\left(\frac{a'}{r}\right)^2 - \left(\frac{a'}{b}\right)^2}{1 - \left(\frac{a'}{b}\right)^2} \right\} \qquad (28)$$

$$\sigma'_z = \frac{2\nu\sigma_o}{\sqrt{3}} \left\{ \left(\frac{c^2}{b}\right) - \alpha' \frac{\left(\frac{a'}{b}\right)^2}{1 - \left(\frac{a'}{b}\right)^2} \right\}$$

where, by analogy with (14),

$$\alpha' = 2 \ln \frac{c}{a'} + 1 - \left(\frac{c^2}{b}\right) \qquad (29)$$

Equations (27) and (28) give the residual stress after reaming to radius a' in an annulus in which loading caused yield to radius c.

3.3.2 Reaming - Incipient Reyield at Radius r = a'

Following the procedure of Section 3.2.2 there results an identical relationship to (19) where a there becomes a':

$$2 \ln \frac{c}{a'} + 1 - \left(\frac{c^2}{b}\right) = 2 \left[1 - \left(\frac{a'^2}{b}\right)\right] = \alpha' \tag{30}$$

Thus, the information contained in Fig. 4 applies also to the reamed hole provided the change in radius is noted.

3.3.3 Reaming where Reyield has occurred

In this case, in addition to the change in radius from a to a', reaming gives rise to a change (increase) in the reyield radius ρ to ρ': the (reyielded) stresses at both original and new bores remaining the same, Fig. 7. The new stresses are found directly from the results of Section 3.2.3.

For the zone $a' \leq r \leq \rho'$

$$\sigma'_r = -\frac{2\sigma_o}{\sqrt{3}} \ln \frac{r}{a'}$$

$$\sigma'_\theta = -\frac{2\sigma_o}{\sqrt{3}} \left[1 + \ln \frac{r}{a'}\right] \tag{31}$$

$$\sigma'_z = -\frac{\sigma_o}{\sqrt{3}} \left[1 + 2 \ln \frac{r}{a'}\right]$$

For the zone $\rho' \leq r \leq c$

$$\sigma'_r = \frac{\sigma_o}{\sqrt{3}} \left\{\left[2 \ln \frac{r}{c} - 1 + \left(\frac{c^2}{b}\right)\right] + 2 \left[\left(\frac{\rho'}{r}\right)^2 - \left(\frac{\rho'}{b}\right)^2\right]\right\}$$

$$\sigma'_\theta = \frac{\sigma_o}{\sqrt{3}} \left\{\left[2 \ln \frac{r}{c} + 1 + \left(\frac{c^2}{b}\right)\right] - 2 \left[\left(\frac{\rho'}{r}\right)^2 + \left(\frac{\rho'}{b}\right)^2\right]\right\} \tag{32}$$

$$\sigma'_z = \frac{\sigma_o}{\sqrt{3}} \left\{\left[2 \ln \frac{r}{c} + \left(\frac{c^2}{b}\right)\right] - 2\nu \left(\frac{\rho'}{b}\right)^2\right\}$$

For the zone $c \leq r \leq b$

$$\sigma'_r = \frac{\sigma_o}{\sqrt{3}} \{[-(\frac{c^2}{r}) + (\frac{c^2}{b})] + 2\,[(\frac{\rho}{r})'^2 - (\frac{\rho}{b})'^2]\}$$

$$\sigma'_\theta = \frac{\sigma_o}{\sqrt{3}} \{[(\frac{c^2}{r}) + (\frac{c^2}{b})] - 2\,[(\frac{\rho}{r})'^2 + (\frac{\rho}{b})'^2]\} \qquad (33)$$

$$\sigma'_z = \frac{\sigma_o}{\sqrt{3}}\, 2\nu\, \{(\frac{c^2}{b}) - 2\,(\frac{\rho}{b})'^2\}$$

3.3.4 Effect of Reaming on Reyield Radius

Following the procedure of Section 3.2.4, there results a similar relationship to (24):

$$2 \ln \frac{a'c}{\rho'^2} + 1 - (\frac{c^2}{b}) = 2\,[1 - (\frac{\rho}{b})'^2] \qquad (34)$$

As before, the information of Fig. 5 holds in this case provided that a and ρ are replaced by a' and ρ'.

The effect of reaming on the change in reyield radius ρ is readily found. By equating the expressions for $(c/b)^2$ from (25) and (34) for the pre-and post-ream situations it is found that

$$\ln \frac{a'}{a} = 2 \ln \frac{\rho'}{\rho} + (\frac{\rho^2}{b}) - (\frac{\rho}{b})'^2 \qquad (35)$$

For b large,

$$\frac{a'}{a} \simeq (\frac{\rho}{\rho})'^2 \qquad (36)$$

and for $\frac{a'}{a} = 1 + \frac{\delta a}{a}$ and $\frac{\rho'}{\rho} = 1 + \frac{\delta \rho}{\rho}$,

$$\frac{\delta \rho}{\rho} \simeq \tfrac{1}{2} \frac{\delta a}{a} \quad . \qquad (37)$$

i.e. a small increase in radius caused by reaming increases the reyielded radius by about half as much.

This effect can be seen in the previous example reworked here with an assumed (and enormous) 10% ream. The circumferential stress distributions before and after reaming are shown in Fig. 7(a), the detail in the reyield region being shown

enlarged in Fig. 7(b). It is clear that the effect of this degree of reaming on the residual hoop stress is small: at more realistic, much smaller, degrees of reaming the changes will be quite inconsequential. Any possible effect of the slightly less beneficial stress distribution on the fatigue process from this point of view would have to be judged negligible.

4. STRAINS

In this Section principal strains for the various loading conditions are given. The format follows that for stresses. In both elastic and plastic regimes in two-dimensional radial flow strains and displacements are very simply related:

$$\epsilon_r = \frac{du_r}{dr} \tag{38}$$

and

$$\epsilon_\theta = \frac{u_r}{r} \tag{39}$$

so that radial displacement is found directly from circumferential strain as:

$$u_r = r\epsilon_\theta \tag{40}$$

For this reason, strains alone are explicitly formulated in the following.

4.1 Loaded Annulus

As before, the application of pressure to the bore gives rise to the three outcomes of interest:

(a) elastic expansion throughout

(b) as above, but with incipient yield at the bore

(c) elasto-plastic expansion

Strains in all regions are readily found from (1) or (6) in conjunction with the appropriate stress substitutions.

4.1.1 Elastic Conditions Throughout

The substitution of (9) into (1) provide the required equations of elastic strain in a pressurised annulus. They are:

$$\epsilon_r = -\frac{p}{E}\frac{(1+\nu)}{1-(\frac{a^2}{b})}\{(\frac{a^2}{r}) - (1-2\nu)(\frac{a^2}{b})\}$$

and (41)

$$\epsilon_\theta = \frac{p}{E}\frac{1+\nu}{1-(\frac{a^2}{b})}\{(\frac{a^2}{r}) + (1-2\nu)(\frac{a^2}{b})\}$$

4.1.2 Incipient Plasticity

At this point (10) provides the value of pressure p to just initiate yielding at the bore. Substitution of (10) into (41) gives

$$\epsilon_r = -\frac{1+\nu}{\sqrt{3}}\frac{\sigma_o}{E}(\frac{a^2}{r})\{1-(1-2\nu)(\frac{a^2}{b})\}$$

and (42)

$$\epsilon_\theta = \frac{1+\nu}{\sqrt{3}}\frac{\sigma_o}{E}(\frac{a^2}{r})\{1+(1-2\nu)(\frac{a^2}{b})\}$$

4.1.3 Strains in Plastic Region

Under conditions of plastic plow, as already noted at (6), the sum of the principal strains is zero. Substitution of (38) and (39) into (6) provides the differential equation

$$\frac{du_r}{dr} + \frac{u_r}{r} = 0 \qquad (43)$$

the solution of which is

$$u_r = \frac{C}{r} \qquad (44)$$

where C is a constant.

From (39) and (44)

$$\epsilon_\theta = \frac{u_r}{r} = \frac{C}{r^2} \qquad (45)$$

Equating (42) and (45) across the elasto-plastic boundary (found by putting $r = c$ and by replacing a by c in (42)), C may be evaluated, leading to

$$\epsilon_r = -\frac{1+\nu}{\sqrt{3}}\frac{\sigma_o}{E}\left(\frac{c^2}{r}\right)\left[1 + (1-2\nu)\left(\frac{c^2}{b}\right)\right]$$

and (46)

$$\epsilon_\theta = \frac{1+\nu}{\sqrt{3}}\frac{\sigma_o}{E}\left(\frac{c^2}{r}\right)\left[1 + (1-2\nu)\left(\frac{c^2}{b}\right)\right]$$

since $\epsilon_r = -\epsilon_\theta$ in the plastic region.

4.1.4 Strains in Elastic Region

Strains here are written down directly from (41), substituting for p the value given by (10):

$$\epsilon_r = -\frac{1+\nu}{\sqrt{3}}\frac{\sigma_o}{E}\left[\left(\frac{c^2}{r}\right) - (1-2\nu)\left(\frac{c^2}{b}\right)\right]$$

(47)

$$\epsilon_\theta = \frac{1+\nu}{\sqrt{3}}\frac{\sigma_o}{E}\left[\left(\frac{c^2}{r}\right) + (1-2\nu)\left(\frac{c^2}{b}\right)\right]$$

A small inconsistency will be noted here arising from the fact that the assumed incompressibility in the plastic region whereby $\epsilon_r = -\epsilon_\theta$ does not carry over into the elastic region. Consequently, radial strain at the elasto-plastic boundary calculated from (46) does not equate with that from (47) at the same position. The difference is proportional to twice the second term in the square brackets which is, in general, relatively small. For ν approaching one half, or for b large, this term becomes insignificant and the discontinuity vanishes.

Figure 8 shows the circumferential and radial strain distributions for the example already given, highlighting the small discontinuities in radial strain at the elasto-plastic boundary $r/a = 2.5$.

4.2 Unloaded Annulus

As before, three outcomes of interest are possible:

(a) elastic unloading throughout

(b) as above, but with incipient reyielding at the bore

(c) as above, but with reyielding

Also as before it is assumed here that an elasto-plastic situation exists prior to unloading.

4.2.1 Elastic Recovery - No Reyielding

Subtraction from (46) and (47) of elastic strains given by (41) with p replaced by (13) provide the sought solutions.

For the zone $a \leq r \leq c$

$$\epsilon_r = -\frac{1+\nu}{\sqrt{3}}\frac{\sigma_o}{E}\left\{\left(\frac{c^2}{r}\right)\left[1+(1-2\nu)\left(\frac{c^2}{b}\right)\right]-\alpha\frac{\left(\frac{a^2}{r}\right)-(1-2\nu)\left(\frac{a^2}{b}\right)}{1-\left(\frac{a^2}{b}\right)}\right\}$$

$$\epsilon_\theta = \frac{1+\nu}{\sqrt{3}}\frac{\sigma_o}{E}\left\{\left(\frac{c^2}{r}\right)\left[1+(1-2\nu)\left(\frac{c^2}{b}\right)\right]-\alpha\frac{\left(\frac{a^2}{r}\right)+(1-2\nu)\left(\frac{a^2}{b}\right)}{1-\left(\frac{a^2}{b}\right)}\right\} \quad (48)$$

For the zone $c \leq r \leq b$

$$\epsilon_r = -\frac{1+\nu}{\sqrt{3}}\frac{\sigma_o}{E}\left\{\left[\left(\frac{c^2}{r}\right)-(1-2\nu)\left(\frac{c^2}{b}\right)\right]-\alpha\frac{\left(\frac{a^2}{r}\right)-(1-2\nu)\left(\frac{a^2}{b}\right)}{1-\left(\frac{a^2}{b}\right)}\right\}$$

$$\epsilon_\theta = \frac{1+\nu}{\sqrt{3}}\frac{\sigma_o}{E}\left\{\left[\left(\frac{c^2}{r}\right)+(1-2\nu)\left(\frac{c^2}{b}\right)\right]-\alpha\frac{\left(\frac{a^2}{r}\right)+(1-2\nu)\left(\frac{a^2}{b}\right)}{1-\left(\frac{a^2}{b}\right)}\right\} \quad (49)$$

where, from (14),

$$\alpha = 2\ln\frac{c}{a}+1-\left(\frac{c^2}{b}\right)$$

4.2.2 Elastic Recovery - Incipient Reyield at Bore

The situation here is similar to that above, except that now some simplifications occur because of (19), whereby

$$\alpha = 2 \ln \frac{c}{a} + 1 - \left(\frac{c^2}{b}\right) = 2 \left[1 - \left(\frac{a^2}{b}\right)\right]$$

For the zone $a \leq r \leq c$

$$\epsilon_r = - \frac{1 + \nu}{\sqrt{3}} \frac{\sigma_o}{E} \left\{\left(\frac{c^2}{r}\right)\left[1 + (1 - 2\nu)\left(\frac{c^2}{b}\right)\right] - 2 \left[\left(\frac{a^2}{r}\right) - (1 - 2\nu)\left(\frac{a^2}{b}\right)\right]\right\}$$

(50)

$$\epsilon_\theta = \frac{1 + \nu}{\sqrt{3}} \frac{\sigma_o}{E} \left\{\left(\frac{c^2}{r}\right)\left[1 + (1 - 2\nu)\left(\frac{c^2}{b}\right)\right] - 2 \left[\left(\frac{a^2}{r}\right) + (1 - 2\nu)\left(\frac{a^2}{b}\right)\right]\right\}$$

For the zone $c \leq r \leq b$

$$\epsilon_r = - \frac{1 + \nu}{\sqrt{3}} \frac{\sigma_o}{E} \left\{\left[\left(\frac{c^2}{r}\right) - (1 - 2\nu)\left(\frac{c^2}{b}\right)\right] - 2 \left[\left(\frac{a^2}{r}\right) - (1 - 2\nu)\left(\frac{a^2}{b}\right)\right]\right\}$$

(51)

$$\epsilon_\theta = \frac{1 + \nu}{\sqrt{3}} \frac{\sigma_o}{E} \left\{\left[\left(\frac{c^2}{r}\right) + (1 - 2\nu)\left(\frac{c^2}{b}\right)\right] - 2 \left[\left(\frac{a^2}{r}\right) + (1 - 2\nu)\left(\frac{a^2}{b}\right)\right]\right\}$$

4.2.3 Unloading giving rise to Reyielded Zone

As before the reyield zone radius is denoted by ρ.

For the zone $a \leq r \leq \rho$

In this reyielded region (44) and (45) again hold. By equating (45) and (50) across the (reyield) elasto-plastic boundary (found by putting $r = \rho$ and by replacing a by ρ in (50)) the constant in (45) may be evaluated. The results are:

$$\epsilon_r = - \frac{1 + \nu}{\sqrt{3}} \frac{\sigma_o}{E} \left\{\left(\frac{c^2}{r}\right)\left[1 + (1 - 2\nu)\left(\frac{c^2}{b}\right)\right] - 2 \left(\frac{\rho^2}{r}\right) \left[1 + (1 - 2\nu)\left(\frac{\rho^2}{b}\right)\right]\right\}$$

and

(52)

$$\epsilon_\theta = - \epsilon_r$$

For the zone $\rho \leq r \leq c$

Strains in this zone follow directly from (50) where a is replaced by ρ.

$$\epsilon_r = -\frac{1+\nu}{\sqrt{3}}\frac{\sigma_o}{E}\left\{\left(\frac{c^2}{r}\right)\left[1+(1-2\nu)\left(\frac{c^2}{b}\right)\right]-2\left[\left(\frac{\rho^2}{r}\right)-(1-2\nu)\left(\frac{\rho^2}{b}\right)\right]\right\}$$

(53)

$$\epsilon_\theta = \frac{1+\nu}{\sqrt{3}}\frac{\sigma_o}{E}\left\{\left(\frac{c^2}{r}\right)\left[1+(1-2\nu)\left(\frac{c^2}{b}\right)\right]-2\left[\left(\frac{\rho^2}{r}\right)+(1-2\nu)\left(\frac{\rho^2}{b}\right)\right]\right\}$$

For the zone $c \leq r \leq b$

As above, strains here are given by (51), after substituting ρ for a:

$$\epsilon_r = -\frac{1+\nu}{\sqrt{3}}\frac{\sigma_o}{E}\left\{\left[\left(\frac{c^2}{r}\right)-(1-2\nu)\left(\frac{c^2}{b}\right)\right]-2\left[\left(\frac{\rho^2}{r}\right)-(1-2\nu)\left(\frac{\rho^2}{b}\right)\right]\right\}$$

(54)

$$\epsilon_\theta = \frac{1+\nu}{\sqrt{3}}\frac{\sigma_o}{E}\left\{\left[\left(\frac{c^2}{r}\right)+(1-2\nu)\left(\frac{c^2}{b}\right)\right]-2\left[\left(\frac{\rho^2}{r}\right)+(1-2\nu)\left(\frac{\rho^2}{b}\right)\right]\right\}$$

As before, Fig. 8 shows the unloaded strain distributions across the annulus for the previous example. Now two discontinuities in radial strain are apparent, one at each of the elasto-plastic boundaries.

4.3 Effect of Reaming

As already discussed under Section 3.3, the effect of reaming (enlarging the bore radius, after cold expansion, from a to a') is readily found by replacing a by a' in the unloading terms in the strain equations of Section 4.2. The changes in strain (pre- and post-reaming) are compared below for the three basic cases considered earlier.

4.3.1 Elastic Recovery - No Reyielding

The strain equations for the pre-reamed case are given by (48) and (49), and for the reamed case by the same equations where a' replaces a. By taking the ratio of the two cases the effect of reaming may be seen. Unfortunately the forms of (48) and (49) do not lend themselves to any simplification when expressed as ratios, except for the case when b is large. In that case

$$\frac{(\epsilon_\theta)_{a'}}{(\epsilon_\theta)_a} = \left(\frac{a'}{a}\right)^2 \frac{\left(\frac{c}{a'}\right)^2 - 1 - 2\ln\frac{c}{a'}}{\left(\frac{c^2}{a}\right) - 1 - 2\ln\frac{c}{a}} = \frac{(\epsilon_r)_{a'}}{(\epsilon_r)_a} \tag{55}$$

independent of radius. The fractional change in strain is the same in both radial and circumferential directions.

4.3.2 Elastic Recovery - Incipient Reyield at Bore

For this case (50) and 51) apply, and for b large,

$$\frac{(\epsilon_\theta)_{a'}}{(\epsilon_\theta)_a} = \frac{\left(\frac{c}{a'}\right)^2 - 2}{\left(\frac{c^2}{a}\right) - 2} = \frac{(\epsilon_r)_{a'}}{(\epsilon_r)_a} \tag{56}$$

at any radius.

4.3.3 Unloading giving rise to Reyielded Zone

For this case (52), (53) and (54) apply. For b large, and at any radius

$$\frac{(\epsilon_\theta)_{a'}}{(\epsilon_\theta)_a} = \frac{\left(\frac{c}{\rho'}\right)^2 - 2}{\left(\frac{c^2}{\rho}\right) - 2} = \frac{(\epsilon_r)_{a'}}{(\epsilon_r)_a} \tag{57}$$

The effect of the ream considered in the example of Section 3.3.4 on strains using strain ratios from (52), (53) and (54) is shown in Fig. 9. For comparison, the result for the ordinate using (57) is 0.82, so that finite annulus geometry must be allowed for.

5. COLDWORKING - EFFECT OF INTERFERENCE

The formulations presented in Sections 3 and 4 for stresses and strains contain the unknowns of pressure (in the case of all-elastic situations) and the elasto-plastic radii c and ρ. In practice the magnitudes of these parameters arise from the interference between mandrel and hole diameters. In this Section the relationships between interference and pressure and interference and elasto-plastic radii are developed.

In the cold-working process, as the mandrel passes through the hole, the interference originally specified is accommodated by

(a) a radial expansion of the bore of the hole and

(b) a radial contraction of the surface of the mandrel.

Thus

$$I = (u)_a - (u_m)_a \tag{58}$$

or

$$\frac{I}{a} = \frac{(u)_a - (u_m)_a}{a} = \lambda \tag{59}$$

where λ is the dimensionless (radial or diametral) interference and the subscript m refers to the mandrel. Since circumferential strain is related to radial displacement by $\epsilon_\theta = u/r$,

$$(\epsilon_\theta)_a = \frac{(u)_a}{a}$$

and

$$\lambda = (\epsilon_\theta)_a - (\epsilon_{\theta m})_a \tag{60}$$

at radius $r = a$. Since the circumferential strain for the annulus has already been found, it remains only to determine that for the mandrel in order to be able to solve (60).

Mandrels are used in practice for some considerable time before wear takes its inevitable toll - typically this corresponds to cold-expanding some thousands of holes. During this time they remain elastic, and their analysis in terms of stresses and strains is simply that of an externally pressurised solid elastic cylinder.

5.1 Loaded Mandrel

The mandrel is represented as a pressurised elastic solid cylinder in plane strain. The principal stresses are given by[5]

$$\sigma_r = \sigma_\theta = - p$$

and (61)

$$\sigma_z = - 2\nu_m p \quad ,$$

all stresses being independent of radius. Circumferential strain is found directly from (1) by substitution of (61) as

$$\epsilon_{\theta m} = - \frac{p}{E_m} (1 + \nu_m)(1 - 2\nu_m) \tag{62}$$

Thus, the circumferential strain is constant at all points throughout the mandrel, including the surface at radius a, the displacement there being given by

$$(u_m)_a = - \frac{p}{E_m} (1 + \nu_m)(1 - 2\nu_m)a$$

5.2 Loaded Annulus

The three basic cases already considered are re-examined below in terms of interference.

5.2.1 Elastic Conditions throughout

Equations (41) for circumferential strain represents this case. Substituting (41) and (62) into (60) gives, with E_m expressed in terms of the modulus ratio $g = E/E_m$, at $r = a$

$$\frac{p}{E} = \frac{\lambda \left(1 - \left(\frac{a^2}{b}\right)\right)}{(1 + \nu)\left[1 + (1 - 2\nu)\left(\frac{a^2}{b}\right)\right] + (1 + \nu_m)(1 - 2\nu_m)\, g \left(1 - \left(\frac{a^2}{b}\right)\right)} \tag{63}$$

Equation (63) defines the interface pressure in terms of the geometric and material properties only. Used in conjunction with (9) and (41), stresses and strains in the annulus may be evaluated directly.

In situations involving interference-fitting of a fastener in a hole it is normal that the plate material remains elastic - interference levels are usually not such as to cause plastic flow. The stresses and strains in such situations are fully described by (9) and (41) in conjunction with (63) when both fastener and annulus are in a state of plane strain.

5.2.2 Incipient Plasticity

The pressure to initiate yield at the bore of the hole has been found (10) as

$$p = \frac{\sigma_o}{\sqrt{3}} \left[1 - \left(\frac{a^2}{b}\right)\right]$$

Substituting this value for p in (63) gives

$$\lambda \frac{E}{\sigma_o} = \frac{1}{\sqrt{3}} \left\{(1 + \nu)\left[1 + (1 - 2\nu)\left(\frac{a^2}{b}\right)\right] + (1 + \nu_m)(1 - 2\nu_m)\, g \left[1 - \left(\frac{a^2}{b}\right)\right]\right\} \quad (64)$$

Equation (64) specifies, for given geometry and material, the level of interference which will just produce yield at the bore of the hole. Thus, (64) determines whether plastic flow will, or will not, occur for a given level of interference.

For the case of common Poisson's ratios and moduli, $\nu = \nu_m$ and $g = 1$, (64) simplifies to

$$\lambda \frac{E}{\sigma_o} = \frac{2}{\sqrt{3}} (1 - \nu^2)$$

Thus, the onset of yield is independent of geometry and is a function only of Poisson's ratio for this particular case only.

5.2.3 Plastic Region – Relationship between λ and c

In the plastic region equations (46) apply. Substituting (46) and (62) into (59) gives, at $r = a$,

$$\lambda = \frac{1 + \nu}{\sqrt{3}} \frac{\sigma_o}{E} \left(\frac{c^2}{a}\right)\left[1 + (1 - 2\nu)\left(\frac{c^2}{b}\right)\right] + \frac{p}{E_m} (1 + \nu_m)(1 - 2\nu_m) \quad (65)$$

The pressure p applied at radius $r = a$ to cause yielding to radius c has already been found (13) as

$$p = \frac{\sigma_o}{\sqrt{3}} \left[2 \ln \frac{c}{a} + 1 - \left(\frac{c^2}{b}\right)\right]$$

Substituting this value for p in (65), putting $E_m = E/g$ and rearranging gives

$$\lambda \frac{E}{\sigma_o} = \frac{1}{\sqrt{3}} \{(1 + \nu)(\frac{c^2}{a})[1 + (1 - 2\nu)(\frac{c^2}{b})] +$$

$$+ (1 + \nu_m)(1 - 2\nu_m)\, g\, [2 \ln \frac{c}{a} + 1 - (\frac{c^2}{a})]\} \qquad (66)$$

Equation (66) provides the sought solution between interference λ and elasto-plastic boundary radius c: unfortunately it is clearly not practical to express c in terms of λ. The effect of interference on the elasto-plastic radius c as a function of geometry b/a is given in Figs. 10 for the case $\nu = \nu_m = 1/3$: in Fig. 10(a) the modulus ratio $g = 1/3$ and in Fig. 10(b), $g = 1$. Comparison of the two sets of graphs shows that the effect of g is not marked, and the same may be said of the effect of geometry - the plastic radius resulting from a given interference is not greatly affected by b/a. The common value of $\lambda E/\sigma_o$ occurring at incipience ($c/a = 1$) for the case $g = 1$, noted in Section 5.2.2, may be seen in Fig. 10(b). Once interference is such as to locate the point of interest below the cluster of curves, full plastic flow has occurred throughout the annulus. This is a situation not usually found in cold-working.

For the example considered earlier, where $c/b = ½$, $b/a = 5$ and $c/a = 2.5$, with $\nu = \nu_m = 1/3$ and $g = 1/3$ (typical of a steel mandrel in an aluminium alloy annulus) Fig. 10(a) (or equation (66)) gives

$$\lambda E/\sigma_o = 5.43$$

With $\sigma_o/E = 0.005$ for a typical aluminium alloy, λ, expressed as a percentage, becomes

$$\lambda = 2.7\%.$$

Thus, in this example, an interference of 2.7% gives rise to an elasto-plastic boundary at one-half of the outside radius. For a more representative interference of perhaps 3% to 4%, the radius of that boundary will be a little larger.

For b large, (66) becomes

$$\lambda \frac{E}{\sigma_o} = \frac{1}{\sqrt{3}} \{(1 + \nu)(\frac{c^2}{a}) + (1 + \nu_m)(1 - 2\nu_m)\, g\, [\ln (\frac{c^2}{a}) + 1]\} \qquad (67)$$

The first term is dominating, so that on a log-log plot a virtual straight line results: this is seen in Figs. 10.

Finally, it should be noted that the relationship between the loaded and unloaded yield radii c and ρ has already been established (25) as

$$2 \ln \frac{ac}{\rho^2} + 1 - \left(\frac{c^2}{b}\right) = 2 \left[1 - \left(\frac{\rho^2}{b}\right)\right] \qquad (25)$$

Thus, for a given interference, c may be found from (66) or Figs. 10, and then ρ from (25) or Fig. 5. All stresses and strains in plane strain cold-worked annuli may then be determined from the appropriate equations in Sections 3 and 4.

6. COMPARISON WITH FINITE ELEMENT ANALYSIS

Finite element analyses have been carried out under two-dimensional plane stress and plane strain conditions[13] and compared with results from a three-dimensional *analysis*[14] *in which* hole diameter was equal to the thickness of the annulus, inner and outer radii and expansions being identical. That comparison showed that the situation in the interior of the three-dimensional annulus was very well described by the two-dimensional results. It is of interest, therefore, to ascertain how well results from the formulations in this report agree with the finite element plane strain predictions.

The finite element anlyses were carried out using the incremental plasticity routines included in ARL's PAFEC computer codes. Apart from the differing theoretical bases (incremental versus deformation plasticity theory) the finite element analyses used the bilinear work-hardening stress-strain relationship indicated below, whereas the present report is based on an elastic/perfectly-plastic relationship. In each case the radius ratio $b/a = 10$ and a 4% interference between the steel mandrel and the hole in the aluminium alloy annulus has been used.

Property	Annulus	Mandrel
Modulus of elasticity (MPa)	69,000	209,000
Poisson's ratio	0.33	0.30
Yield stress (MPa)	480	
Work Hardening slope (MPa)	1,200	(finite element analysis only)

6.1 **Plane Strain Analysis (this report)**

In any given case it will usually be known whether plastic flow is to be expected. If in doubt, the determining equation (64) may be used. In the present case the value of the right side of (64) is 0.6%, so that an applied interference λ of 4% will certainly cause yield. Reference to Fig. 10(a) or the solving of (66) by trial and error for c/a gives

$$\frac{c}{a} = 2.645$$

Reference to Fig. 5 indicates that reyielding is to be expected and (25) may be used to solve precisely (also by trial and error) for ρ. Here

$$\frac{\rho}{a} = 1.255$$

The several radius ratios required in solving the stress and strain equations are then noted. These are:

$$\frac{c}{b} = 0.265 \qquad \frac{\rho}{a} = 1.255$$

$$\frac{c}{\rho} = 2.108 \qquad \frac{\rho}{b} = 0.126$$

and the required solutions are then calculated from the following equations for the cases indicated.

For the loaded case

Radial Zone	Stress	Strain
$a \leq r \leq c$	(12)	(46)
$c \leq r \leq b$	(15)	(47)

For the unloaded case

Radial Zone	Stress	Strain
$a \leq r \leq \rho$	(21)	(52)
$\rho \leq r \leq c$	(22)	(53)
$c \leq r \leq b$	(24)	(54)

6.2 Comparison of 2-D Solutions

Loaded and unloaded stress and strain predictions from the finite element solutions and those calculated as indicated above are compared in Figs. 11, 12 and 13.

It is seen that:

(a) circumferential and radial stresses show good agreement for both loaded and unloaded situations.

(b) out-of-plane stresses do not agree well, particularly near the hole.

(c) circumferential strains agree well for both loaded and unloaded cases: radial strains do not.

Notice that, for this case where a/b is relatively small, the step changes in σ_z and ϵ_r at the elasto-plastic boundaries are not discernible.

As noted above, as well as the differing theoretical basis between the analyses, the stress-strain relationships also differ in the plastic region. It is considered that, in spite of these differences, the approximate theory given here gives good predictions for those parameters likely to be of major interest - in-plane stresses and radial displacement (i.e. circumferential strain). For the purpose of obtaining at least a first estimate, use of the present formulations would appear to be worthwhile.

7. CONCLUSIONS

Closed-form expressions, which are easily evaluated, have been given for the quantities of interest associated with the cold working of holes. Although these have been based on a simplified theory of plasticity, the results agree well with those from a finite element analysis using the exact (incremental) theory. The differences which do occur are either small in magnitude or affect quantities of secondary interest only. The effect of reaming in relieving residual stresses is minimal.

13. R.P. Carey. Computed stress and strain distributions under interference fit and after cold-working. Dept. Defence, Aeronautical Research Laboratories, Structures Technical Memorandum 466, August 1987.

14. R.P. Carey. Three dimensional computation of stress, strain and strain energy density under interference-fit and after cold-working of holes. Dept. Defence, Aeronautical Research Laboratory, Structures Technical Memorandum 478, January 1988.

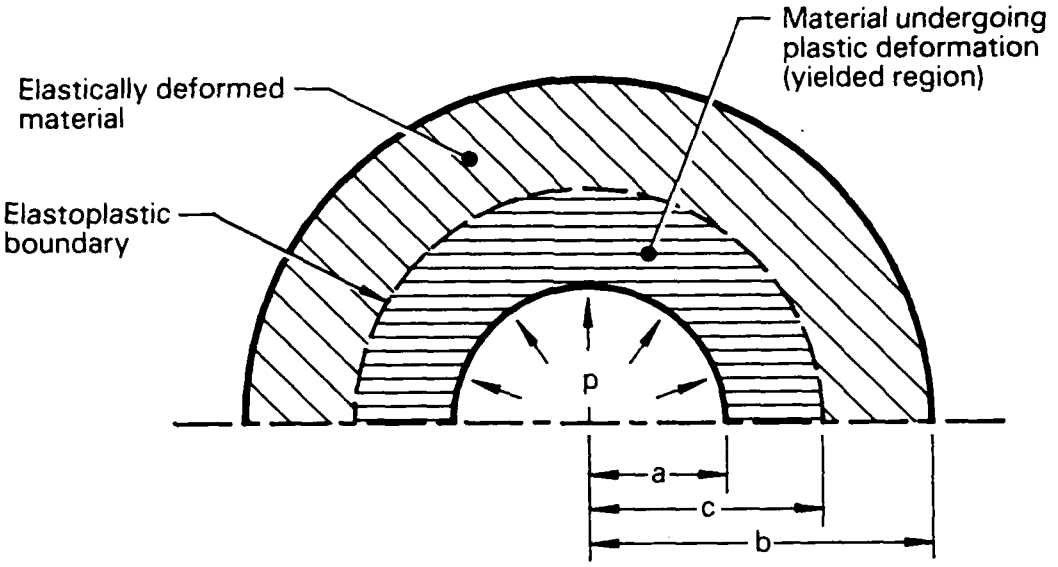

(a) Hole loaded by internal pressure (loaded)

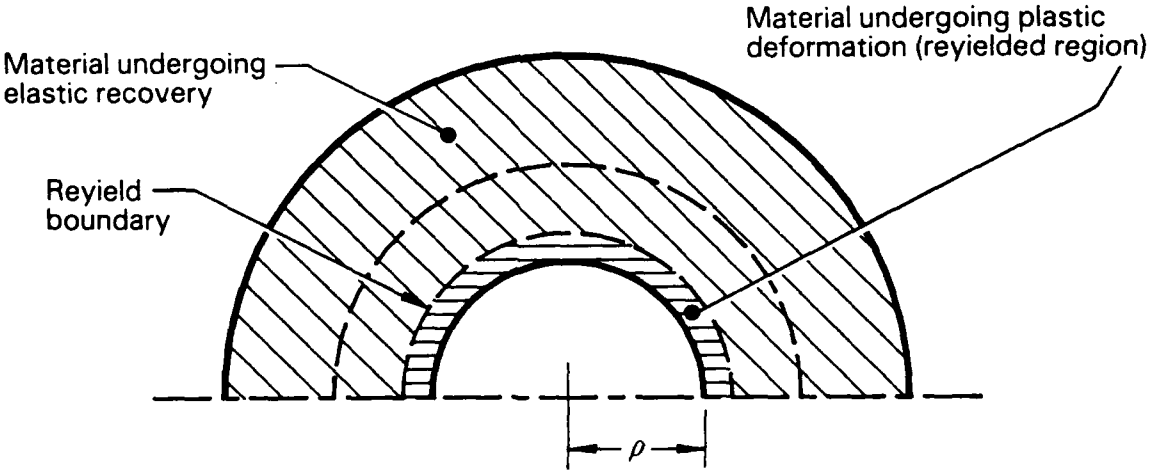

(b) As above after removal of internal pressure (unloaded)

FIG. 1 IDEALISATION OF HOLE COLD-EXPANSION

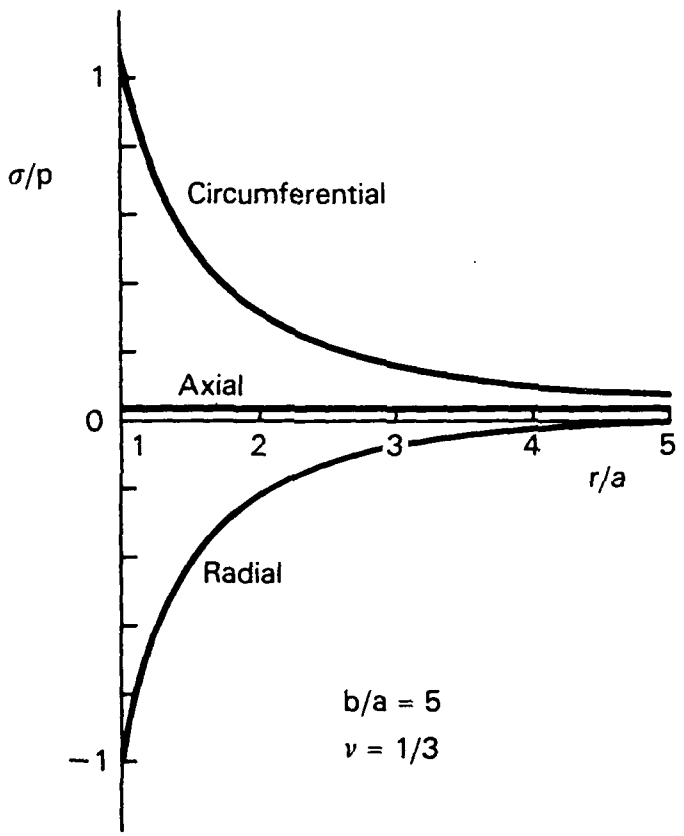

FIG 2. STRESSES IN A PRESSURISED ELASTIC ANNULUS

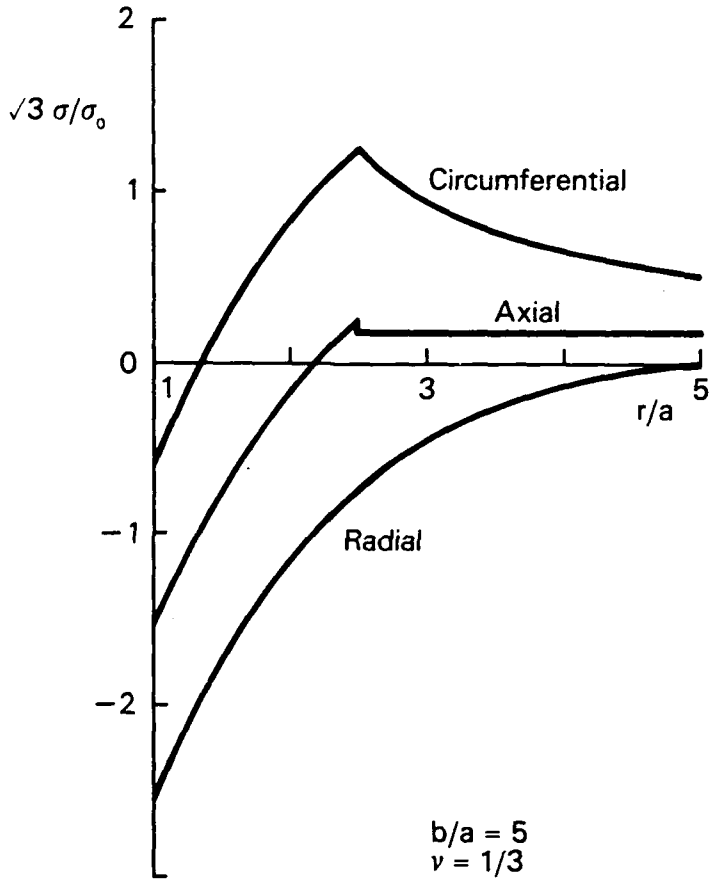

FIG 3. STRESSES IN AN ELASTOPLASTIC LOADED ANNULUS

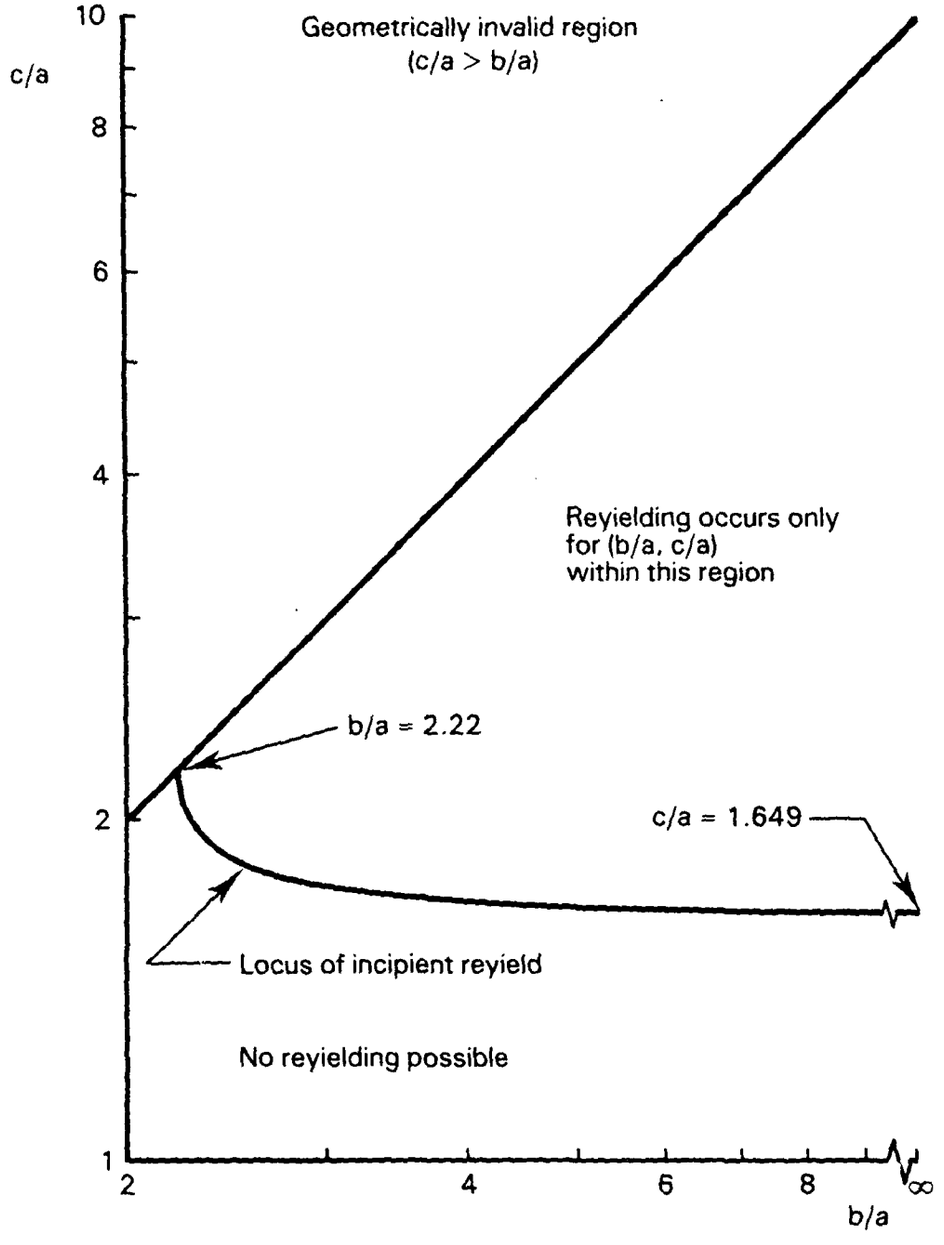

FIG. 4 EFFECT OF GEOMETRY a/b ON YIELD RADIUS c/a

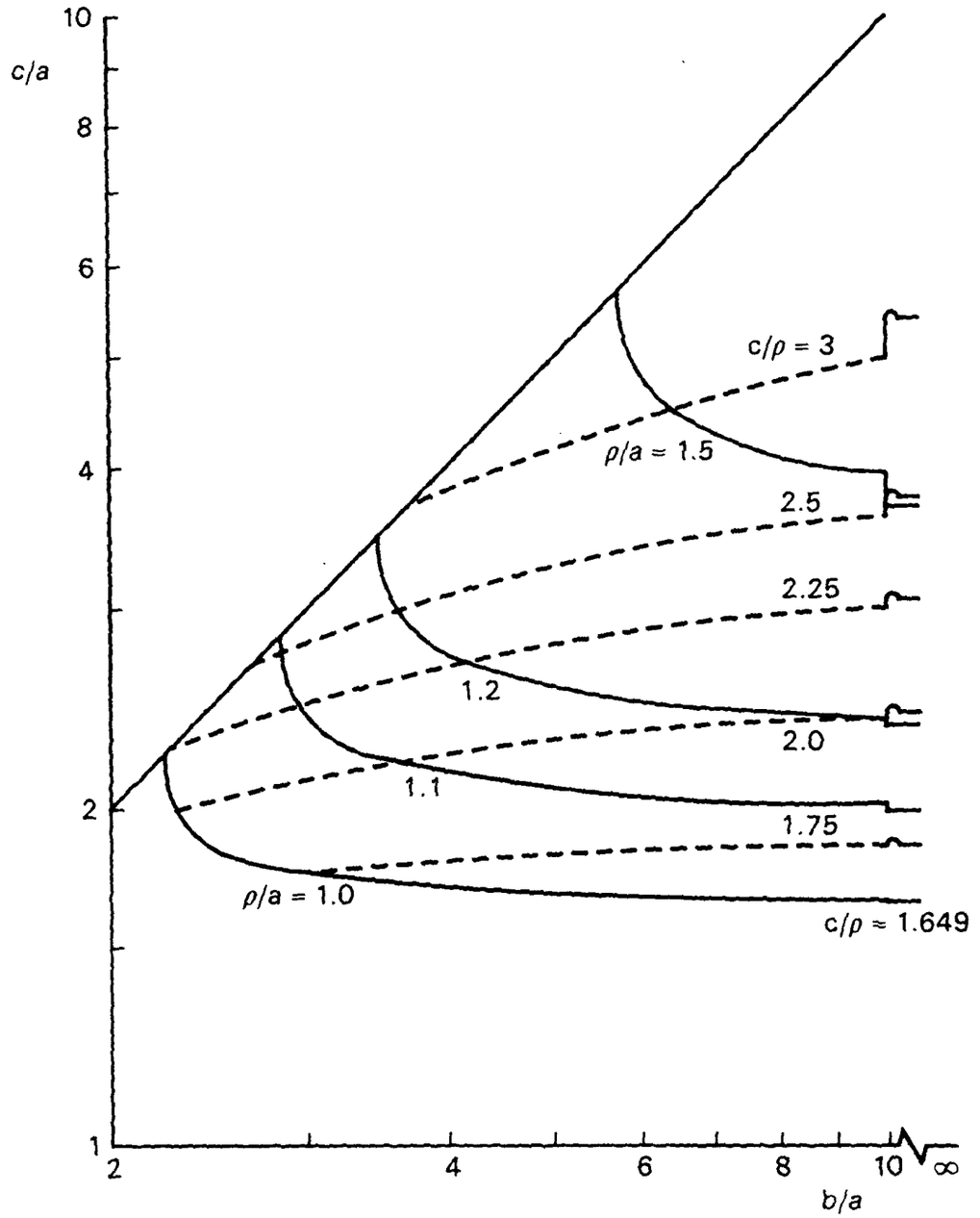

FIG. 5 RELATION BETWEEN YIELD AND REYIELD RADII c/a AND ρ/a IN TERMS OF GEOMETRY b/a

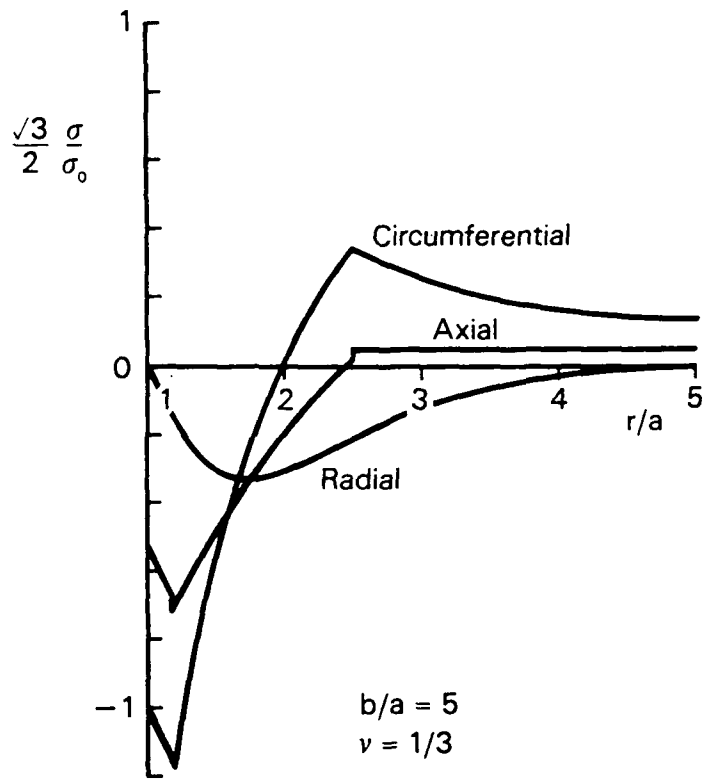

FIG. 6 RESIDUAL STRESSES IN AN ELASTOPLASTICALLY LOADED ANNULUS (AFTER UNLOADING)

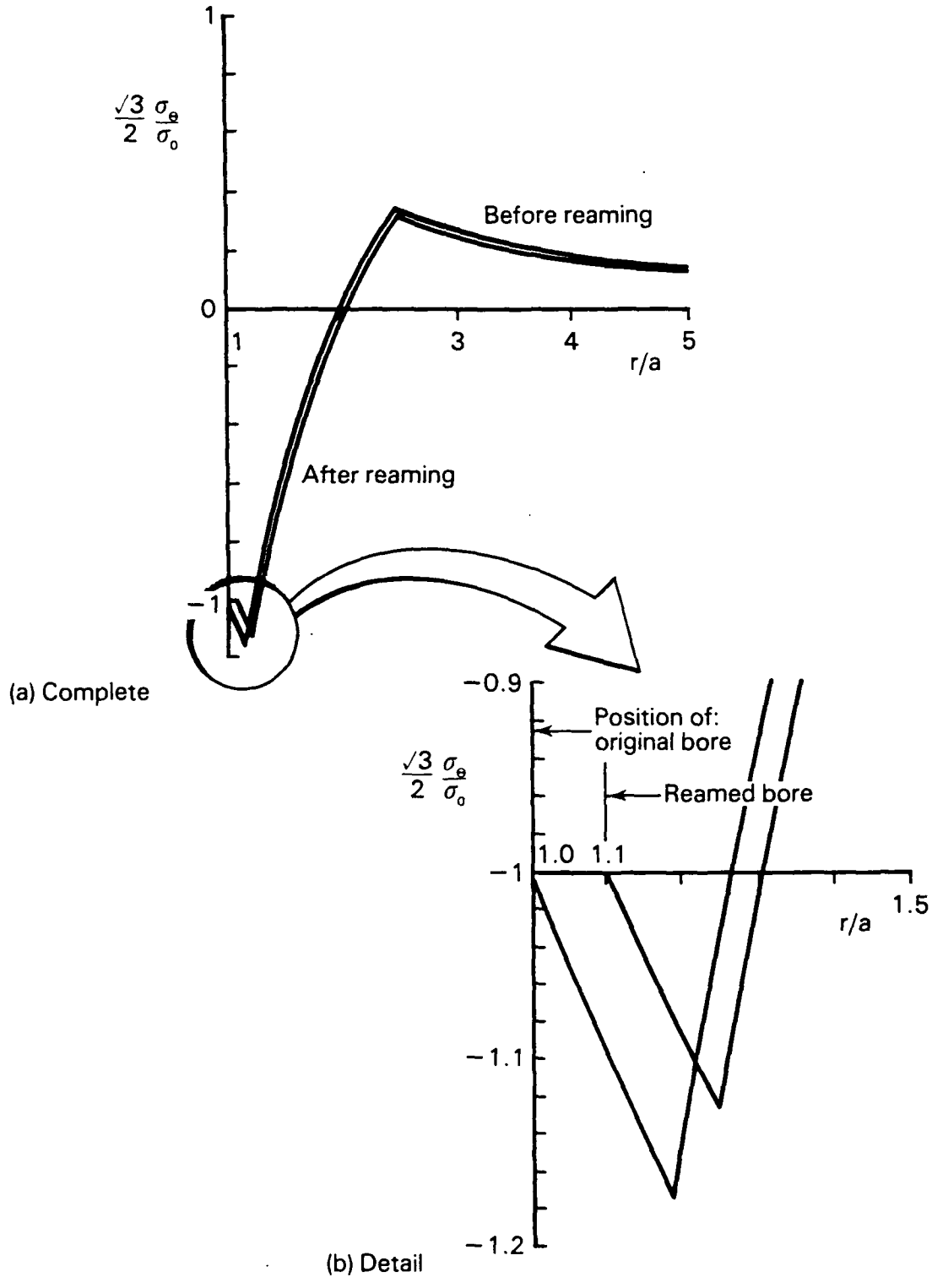

FIG. 7 EFFECT OF REAMING ON RESIDUAL CIRCUMFERENTIAL STRESS

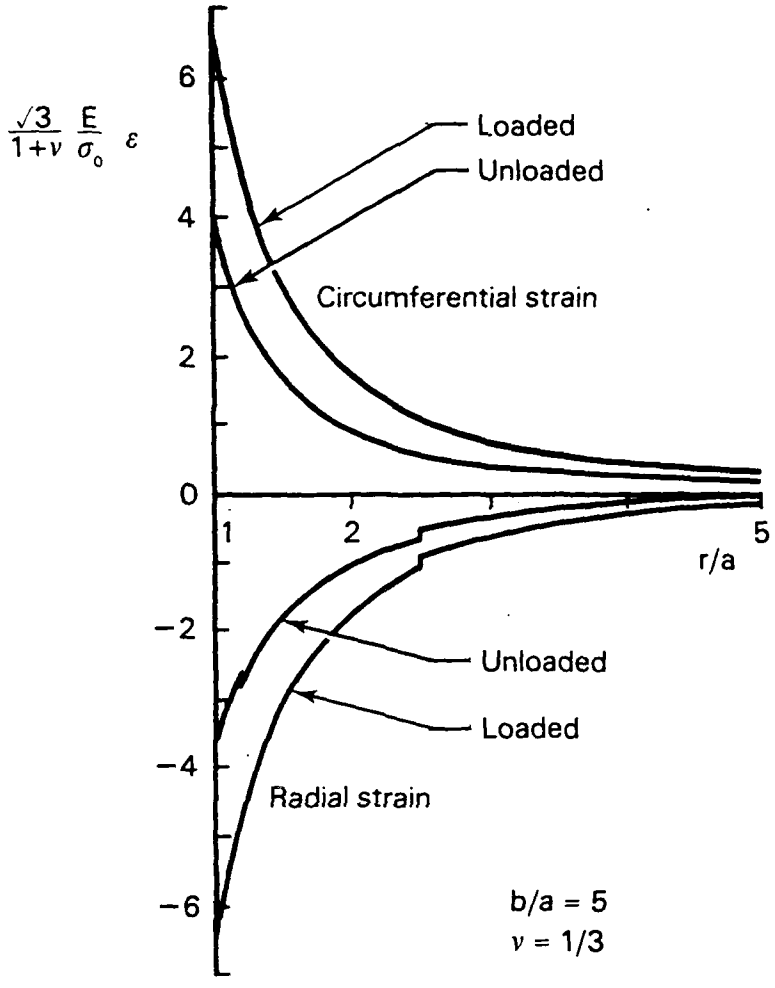

FIG. 8 STRAINS IN ANNULUS UNDER LOADED AND UNLOADED CONDITIONS

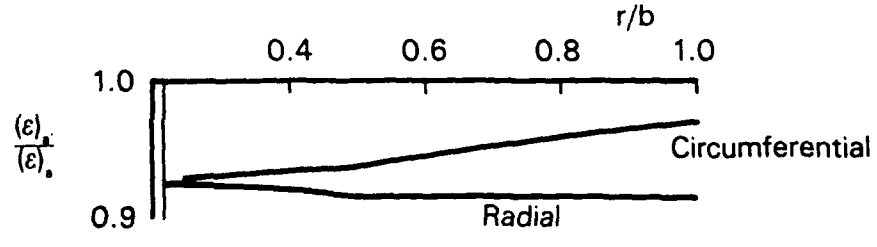

FIG. 9 CHANGE IN STRAIN RESULTING FROM 10% REAMING

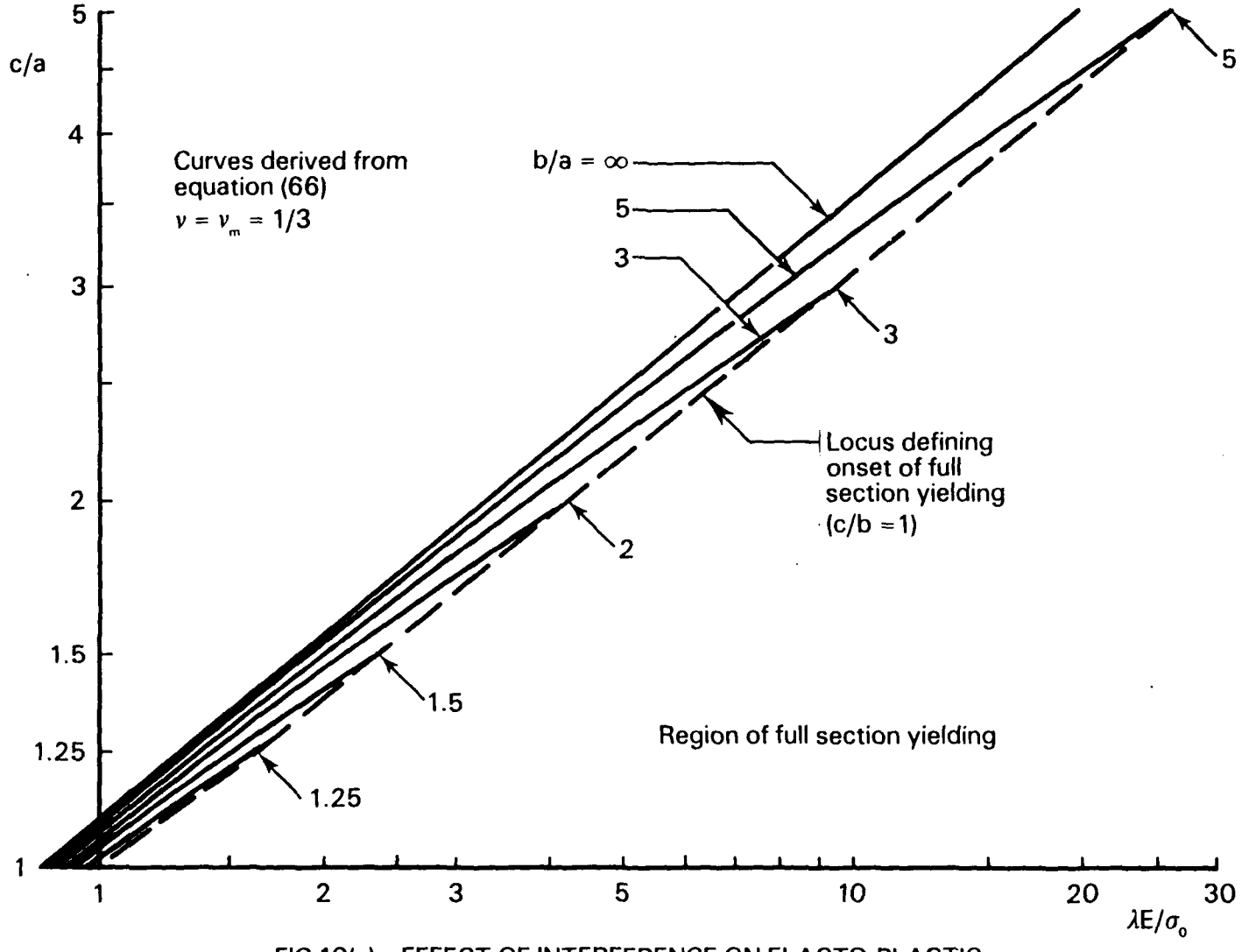

FIG 10(a) EFFECT OF INTERFERENCE ON ELASTO-PLASTIC RADIUS (g = 1/3)

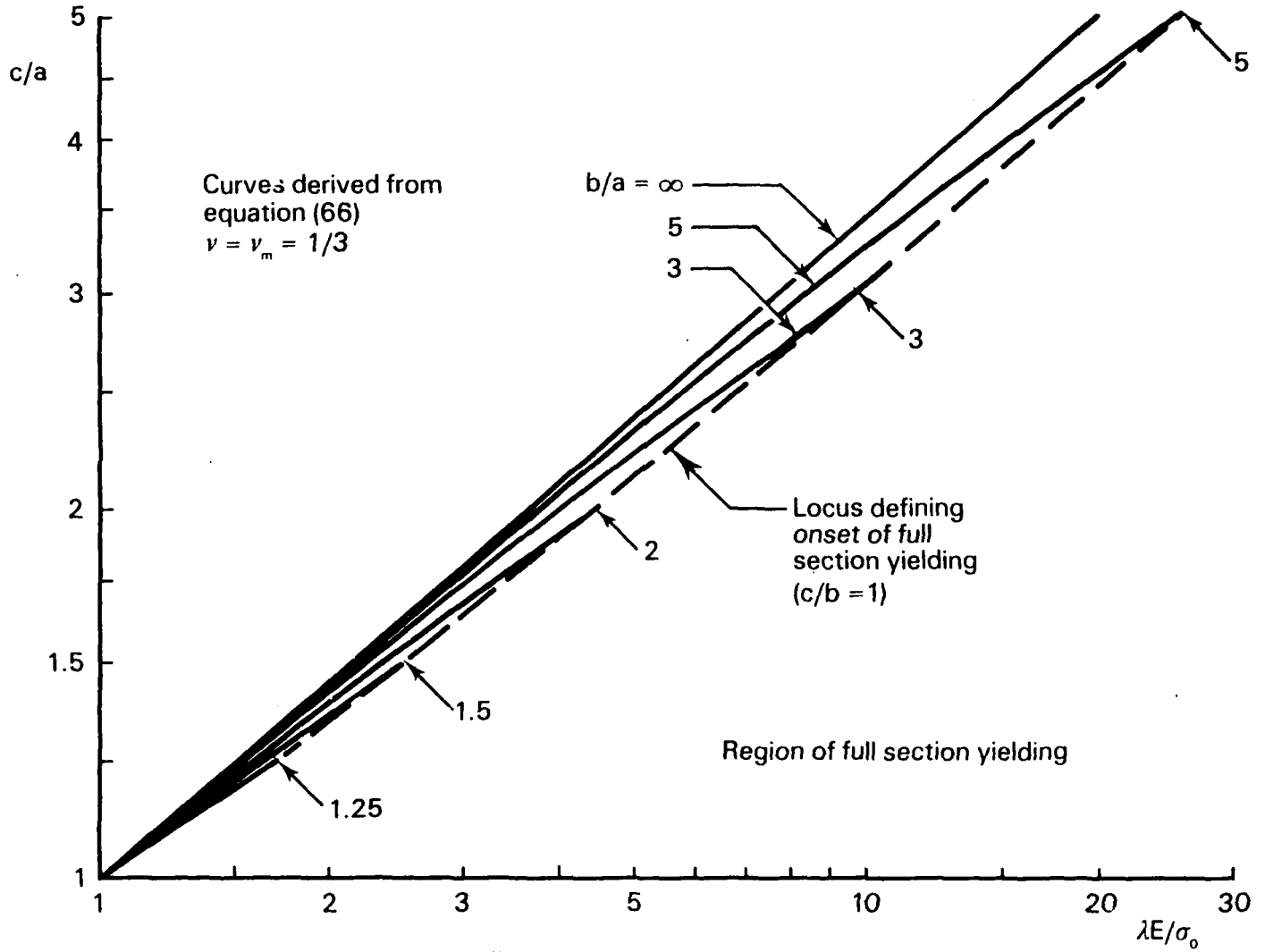

FIG 10(b) EFFECT OF INTERFERENCE ON ELASTO-PLASTIC RADIUS (g = 1)

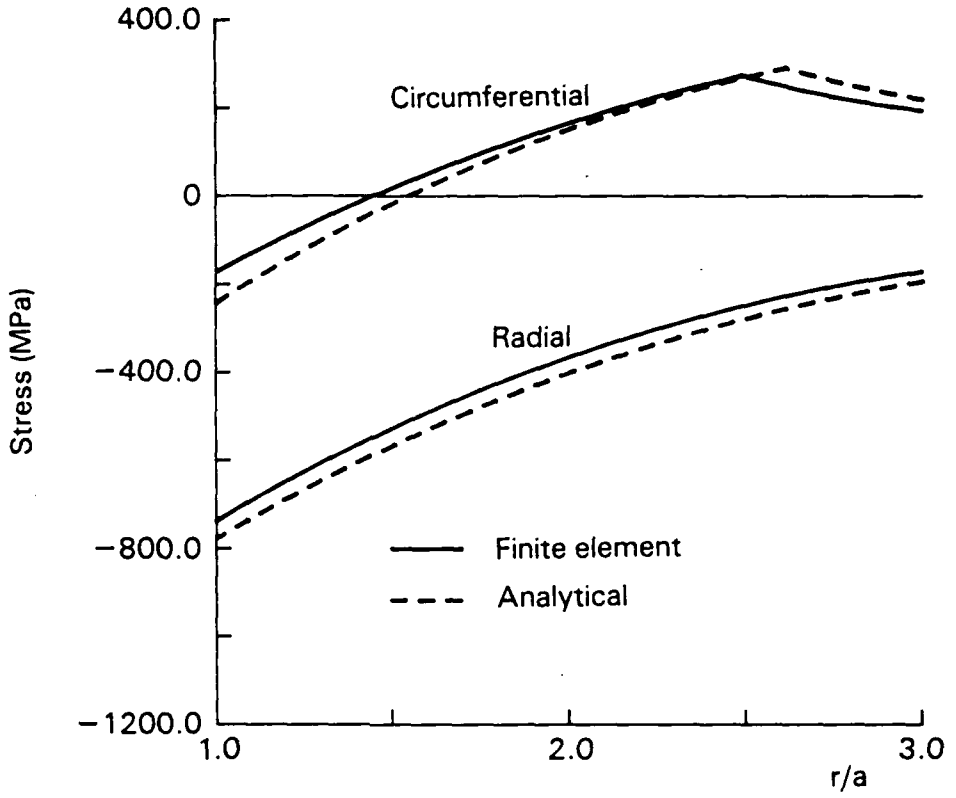

(a) Loaded

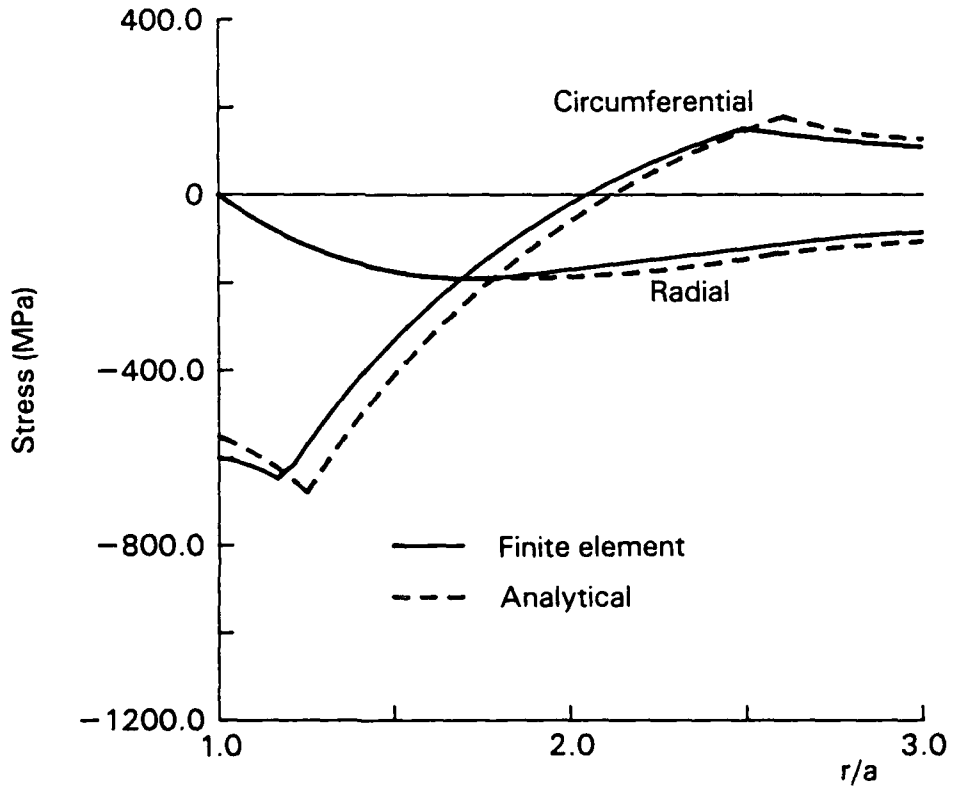

(b) Unloaded

FIG. 11 COMPARISON OF IN-PLANE FINITE ELEMENT AND ANALYTICAL STRESSES

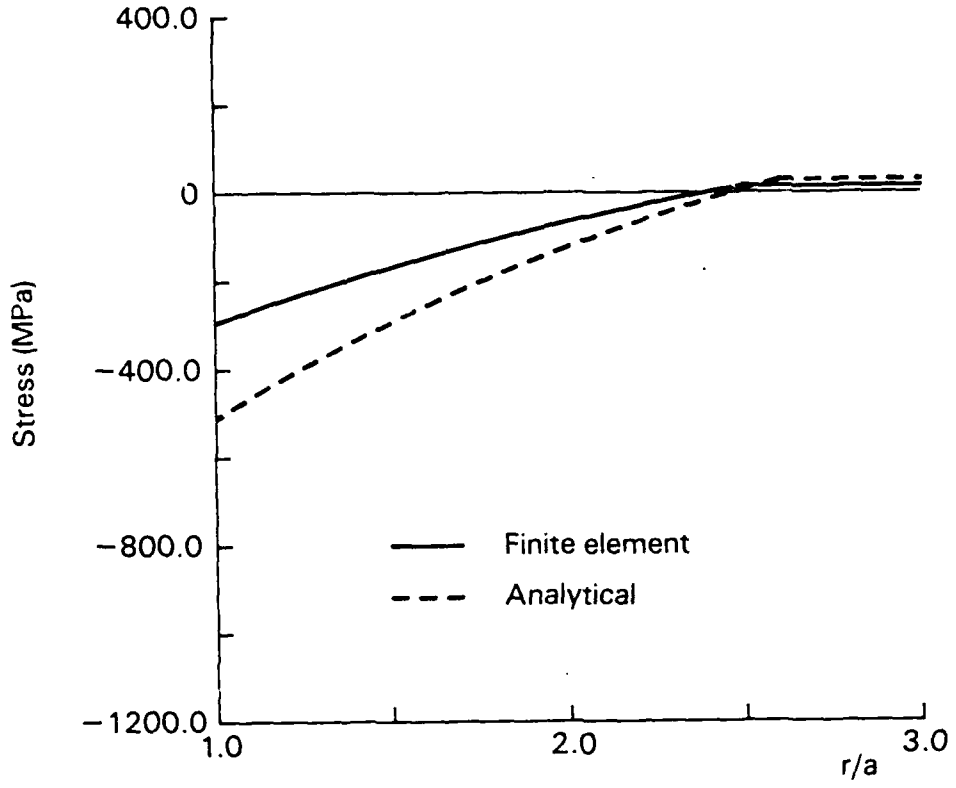

(a) Loaded

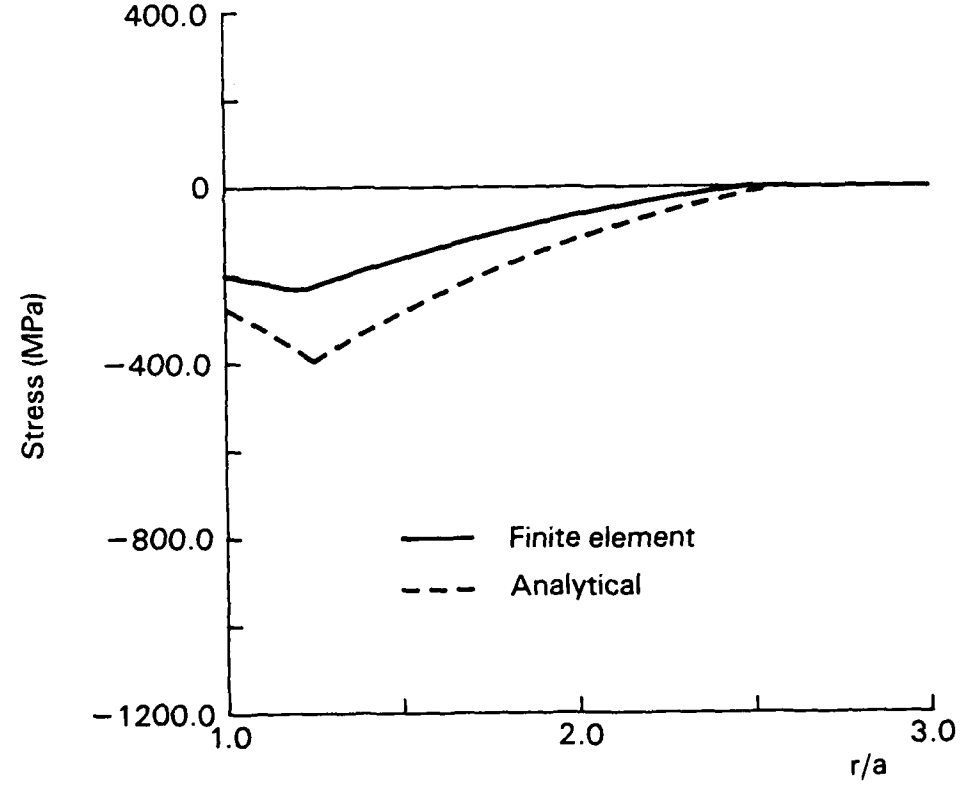

(b) Unloaded

FIG. 12 COMPARISON OF OUT-OF-PLANE FINITE ELEMENT AND ANALYTICAL STRESSES

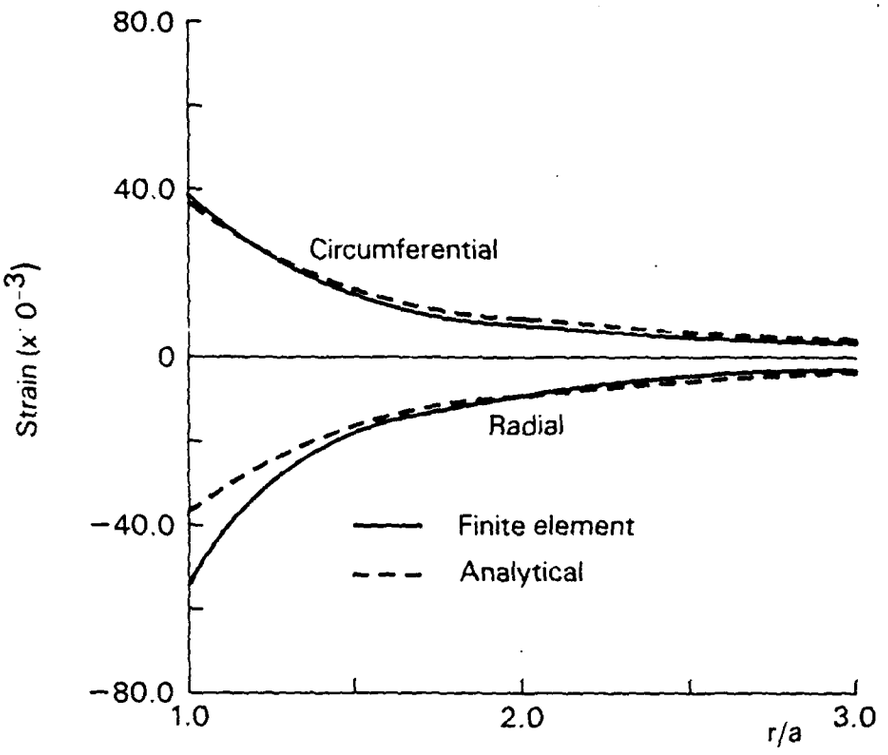

(a) Loaded

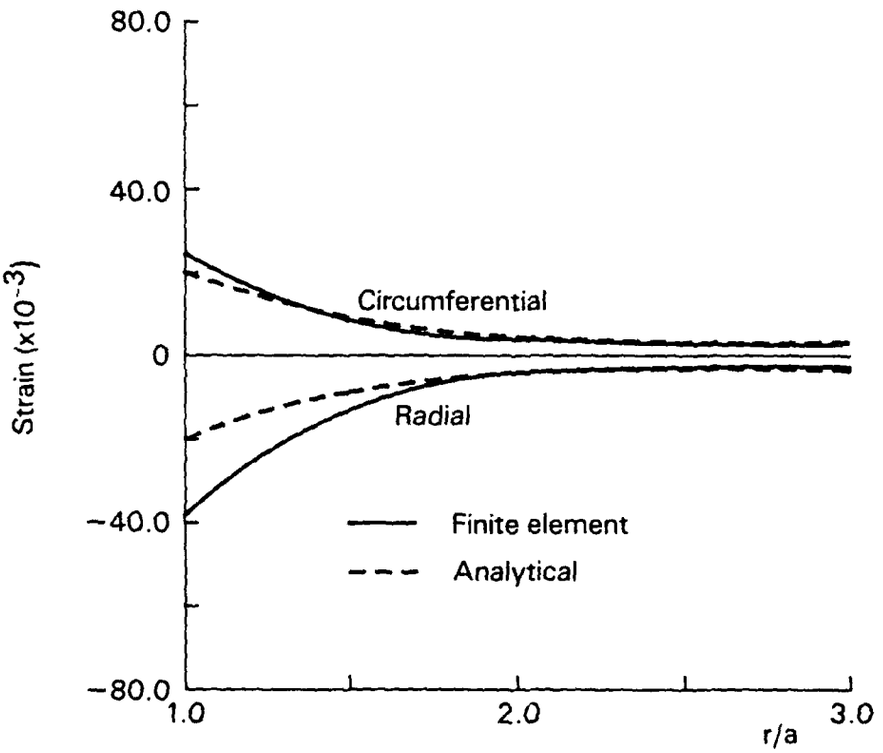

(b) Unloaded

FIG. 13 COMPARISON OF FINITE ELEMENT AND ANALYTICAL STRAINS

DISTRIBUTION

AUSTRALIA

Department of Defence

Defence Central
- Chief Defence Scientist
- Assist Chief Defence Scientist, Operations (shared copy)
- Assist Chief Defence Scientist, Policy (shared copy)
- Director, Departmental Publications
- Counsellor, Defence Science (London) (Doc Data Sheet Only)
- Counsellor, Defence Science (Washington) (Doc Data Sheet Only)
- S.A. to Thailand MRD (Doc Data Sheet Only)
- S.A. to the DRC (Kuala Lumpur) (Doc Data Sheet Only)
- OIC TRS, Defence Central Library
- Document Exchange Centre, DISB (18 copies)
- Joint Intelligence Organisation
- Librarian H Block, Victoria Barracks, Melbourne
- Director General - Army Development (NSO) (4 copies)
- Defence Industry and Materiel Policy, FAS

Aeronautical Research Laboratory
- Director
- Library
- Chief Aircraft Structures
- Divisional File Aircraft Structures
- Author: G.S. Jost
- B.C. Hoskin
- D.G. Ford
- C.K. Rider
- J.M. Finney
- J.G. Sparrow
- R. Jones
- D.S. Saunders
- L.R. Gratzer
- R.P. Carey
- G. Clark

Materials Research Laboratory
- Director/Library

Defence Science & Technology Organisation - Salisbury
- Library

Navy Office
- Navy Scientific Adviser (Doc Data sheet only)

Army Office
- Scientific Adviser - Army (Doc Data sheet only)
- Engineering Development Establishment, Library

Air Force Office
Air Force Scientific Adviser (Doc Data sheet only)
Aircraft Research and Development Unit
Library
Engineering Division Library
Director General Aircraft Engineering - Air Force

Department of Transport & Communication
Library

Statutory and State Authorities and Industry
Aero-Space Technologies Australia, Manager/Librarian (2 copies)
Australian Airlines, Library
Qantas Airways Limited
Ansett Airlines of Australia, Library
BHP, Melbourne Research Laboratories
Hawker de Havilland Aust Pty Ltd, Victoria, Library
Hawker de Havilland Aust Pty Ltd, Bankstown, Library
Civil Aviation Authority

Universities and Colleges
Adelaide
Barr Smith Library

Flinders
Library

La Trobe
Library

Melbourne
Engineering Library

Monash
Hargrave Library

Newcastle
Library

New England
Library

Sydney
Engineering Library
Dr G.P. Steven, Dept. of Aeronautical Engineering,

NSW
Physical Sciences Library
Library, Australian Defence Force Academy

Queensland
Library

Tasmania
Engineering Library

Western Australia
Library

RMIT
Library

University College of the Northern Territory
Library

CANADA
CAARC Coordinator Structures

NRC
Aeronautical & Mechanical Engineering, Library
Division of Mechanical Engineering, Library

Universities and Colleges
Toronto
Institute for Aerospace Studies

FRANCE
ONERA, Library

INDIA
CAARC Coordinator Structures
Defence Ministry, Aero Development Establishment, Library
Hindustan Aeronautics Ltd, Library
National Aeronautical Laboratory, Information Centre

ISRAEL
Technion-Israel Institute of Technology

JAPAN
National Aerospace Laboratory
National Research Institute for Metals, Fatigue Testing Div.
Institute of Space and Astronautical Science, Library

NETHERLANDS
National Aerospace Laboratory (NLR), Library

NEW ZEALAND
Defence Scientific Establishment, Library
RNZAF
Transport Ministry, Airworthiness Branch, Library

Universities
Canterbury
Library

SINGAPORE
Director, Defence Materials Organisation

SWEDEN
Aeronautical Research Institute, Library

SWITZERLAND
F&W (Swiss Federal Aircraft Factory)

UNITED KINGDOM
Ministry of Defence, Research, Materials and Collaboration
CAARC, Secretary
Royal Aircraft Establishment
Bedford, Library
Farnborough, Library
National Physical Laboratory, Library
National Engineering Laboratory, Library
British Library, Document Supply Centre
CAARC Co-ordinator, Structures
Aircraft Research Association, Library

British Aerospace
Kingston-upon-Thames, Library
Hatfield-Chester Division, Library
Short Brothers Ltd, Technical Library

Universities and Colleges
Bristol
Engineering Library

Cambridge
Library, Engineering Department
Whittle Library

Nottingham
Science Library

Southamption
Library

Strathclyde
Library

Cranfield Inst. of Technology
Library

Imperial College
Aeronautics Library

UNITED STATES OF AMERICA
NASA Scientific and Technical Information Facility
Boeing Company
Mr W.E. Binz

Mr J.C. McMillan
Lockheed-California Company
Lockheed Missiles and Space Company
Lockheed Georgia
McDonnell Aircraft Company, Library

SPARES (25 copies)
TOTAL (148 copies)

AL 149 DEPARTMENT OF DEFENCE

DOCUMENT CONTROL DATA

PAGE CLASSIFICATION: UNCLASSIFIED

PRIVACY MARKING:

1a. AR NUMBER	1b. ESTABLISHMENT NUMBER	2. DOCUMENT DATE	3. TASK NUMBER
AR-005-548	ARL-STRUC-R-434	SEPTEMBER 1988	DST 87/039

4. TITLE
STRESSES AND STRAINS IN A COLD-WORKED ANNULUS

5. SECURITY CLASSIFICATION (PLACE APPROPRIATE CLASSIFICATION IN BOX(S) IE. SECRET (S), CONF.(C) RESTRICTED (R), UNCLASSIFIED (U)).

DOCUMENT	TITLE	ABSTRACT
U	U	U

6. NO. PAGES: 54

7. NO. REFS.: 14

8. AUTHOR(S)

G.S. Jost

9. DOWNGRADING/DELIMITING INSTRUCTIONS

Not applicable.

10. CORPORATE AUTHOR AND ADDRESS

AERONAUTICAL RESEARCH LABORATORY
P.O. BOX 4331, MELBOURNE VIC 3001

11. OFFICE/POSITION RESPONSIBLE FOR:

SPONSOR DSTO

SECURITY

DOWNGRADING

APPROVAL DARL

12. SECONDARY DISTRIBUTION (OF THIS DOCUMENT)

Approved for public release.

OVERSEAS ENQUIRIES OUTSIDE STATED LIMITATIONS SHOULD BE REFERRED THROUGH DOCUMENT EXCHANGE CENTRE, DEFENCE INFORMATION SERVICES BRANCH, DEPARTMENT OF DEFENCE, CAMPBELL PARK, CANBERRA, ACT 2601

13a. THIS DOCUMENT MAY BE ANNOUNCED IN CATALOGUES AND AWARENESS SERVICES AVAILABLE TO....

No limitations.

13b. CITATION FOR OTHER PURPOSES (IE. CASUAL ANNOUNCEMENT) MAY BE [X] UNRESTRICTED OR [ ] AS FOR 13a.

14. DESCRIPTORS

Stresses
Strains
Cold working
Interference-fitting
Elasticity
Plasticity

15. DRDA SUBJECT CATEGORIES

0046E
0051C

16. ABSTRACT Analytically-derived plane strain stresses and strains in an annulus pressurised sufficiently to cause plastic flow are given. Unloading giving rise to reyielding around the bore is then examined, along with the effect of reaming. Cold-working is then included in the analysis in terms of interference between mandrel and hole. Finally, comparisons of stress and strain predictions are made with those from a finite element analysis.

PAGE CLASSIFICATION
UNCLASSIFIED
PRIVACY MARKING

THIS PAGE IS TO BE USED TO RECORD INFORMATION WHICH IS REQUIRED BY THE ESTABLISHMENT FOR ITS OWN USE BUT WHICH WILL NOT BE ADDED TO THE DISTIS DATA UNLESS SPECIFICALLY REQUESTED.

16. ABSTRACT (CONT.)

17. IMPRINT

AERONAUTICAL RESEARCH LABORATORY, MELBOURNE

18. DOCUMENT SERIES AND NUMBER	19. COST CODE	20. TYPE OF REPORT AND PERIOD COVERED
Aircraft Structures Report 434	241160	

21. COMPUTER PROGRAMS USED

22. ESTABLISHMENT FILE REF.(S)

B2/91

23. ADDITIONAL INFORMATION (AS REQUIRED)